rss_ringoccs: User Guide
V1.1

Richard G. French*, Sophia R. Flury, Jolene W. Fong,
Ryan J. Maguire, and Glenn J. Steranka

Cassini Radio Science Team Leader,
rfrench@wellesley.edu

February 5, 2019

Contents

List of Figures

List of Tables

1 Introduction

The Cassini Radio Science Subsystem (RSS) was used during the Cassini orbital tour of Saturn to observe a superb series of ring occultations that resulted in high-resolution, high-SNR radial profiles of Saturn's rings at three radio wavelengths: 13 cm (S band), 3.6 cm (X band), and 0.9 cm (Ka band). Radial optical depth profiles of the rings at 1- and 10-km resolution produced by Essam Marouf of the Cassini RSS team, using state-of-the-art signal processing techniques to remove diffraction effects, are available on the NASA Planetary Data System (PDS).[1] These archived products are likely to be quite adequate for many ring scientists, but for those who wish to generate their own diffraction-reconstructed ring profiles from Cassini RSS observations, we provide `rss_ringoccs`: a suite of Python-based analysis tools for radio occultations of planetary rings.[2]

The purpose of `rss_ringoccs` is to enable scientists to produce "on demand" radial optical depth profiles of Saturn's rings from the raw RSS data, without requiring deep familiarity with the complex processing steps involved in calibrating the data and accounting for the effects of diffraction. The code and algorithms are extensively documented, providing a starting point for users who wish to test, refine, or optimize the straightforward methods we have employed. Our emphasis has been on clarity, sometimes at the expense of programming efficiency and execution time. `rss_ringoccs` does an excellent job of reproducing existing RSS processed ring occultation data already present on NASA's PDS Ring-Moon Systems Node – detailed comparisons of representative examples of our results with those on the PDS are presented below in Section 5.1. However, we make no claim to having achieved the state-of-the-art in every respect. In a project this complex, bugs may well be present, and we encourage users to report any errors, augment our algorithms, and share these improvements so that they can be incorporated in future editions of `rss_ringoccs`.

This document provides an introduction to RSS ring occultations, directs users to required and recommended reading, describes in detail how to set up `rss_ringoccs`, and explains how to obtain RSS data files and auxiliary files required by the software. It provides an overview of the processing pipeline, from raw data to final high-resolution radial profiles of the rings, and guides users through a series of simple examples to illustrate the use of `rss_ringoccs`. The algorithms and code are validated by comparison with Voyager and Saturn RSS results on the PDS archive, and with analytical results. Finally, it includes practical considerations for users, and benchmarks of program execution time.

1.1 Getting help

`rss_ringoccs` is easy to install and use, but if you have questions along the way please don't hesitate to get in touch with us. We recommend that you post an issue to the `rss_ringoccs` repository[3] so that other users can join in the conversation, but you are also free to contact the lead author of the project at the email address on the title page of this document. For reference, we provide detailed documentation of the software online at `https://rss-ringoccs.readthedocs.io/en/master/`.

[1] `https://pds-rings.seti.org/cassini/rss/index.html`

[2] `rss_ringoccs` may be found from `https://github.com/NASA-Planetary-Science/rss_ringoccs`

[3] `https://github.com/NASA-Planetary-Science/rss_ringoccs/issues`

1.2 What is an RSS ring occultation?

Simply put, an RSS ring occultation occurs when a radio signal transmitted from a spacecraft's High Gain Antenna (HGA) passes through the rings on the way to a Deep Space Network (DSN) receiving antenna on Earth. The received signal at Earth is affected by interactions of the radio signal with the swarm of ring particles, including attenuation, scattering, Doppler-shifting of the signal, and diffraction. We refer to the process of compensating for diffraction to obtain the intrinsic radial optical depth profile of the rings as diffraction reconstruction or Fresnel inversion, since the reconstruction process is based on the mathematical principles of Fresnel optics.

1.3 Overview of Cassini RSS ring observations

Over the course of the Cassini orbital tour of Saturn, the geometry of RSS ring occultations varied due both to changes in the orbiter's trajectory and to the aspect of the rings as seen from Earth during Saturn's orbit around the Sun. The opening angle of Saturn's rings as a function of time as seen from Earth is shown below in **Fig. 1**.

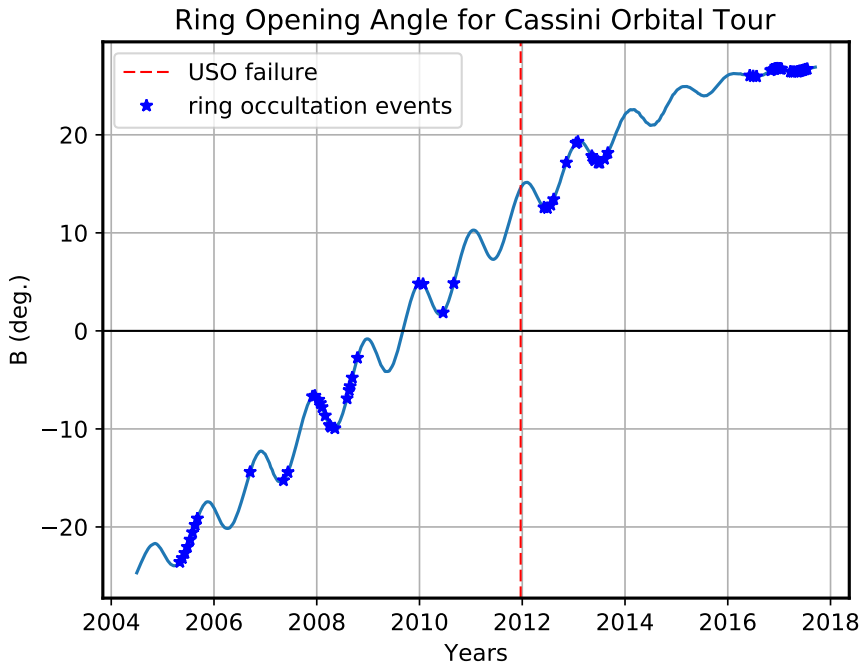

Fig. 1: Ring Opening angle (B) vs. Time. Dark line indicates an opening angle of $B = 0$ where the ring system is edge-on. In 2012, the on-board ultra-stable oscillator (USO) failed, complicating diffraction reconstruction thereafter.

Individual occultations are identified by the Cassini rev number n, corresponding roughly to the n^{th} orbit of Cassini around Saturn, during which the occultation occurred. During the ingress portion of an occultation, the orbital radius of the intercept point in the ring plane of the incident ray from the spacecraft decreases with time; the radius increases with time during the egress portion of an occultation. During a diametric occultation, the ingress and egress portions of the occultation are interrupted by passage of the spacecraft behind the planet itself as seen from Earth, resulting in an atmospheric occultation. The view from Earth of the ingress and egress portions of a diametric occultation on Rev 7 is

shown in **Fig. 2.1**. During a chord occultation, the ingress and egress occultations are contiguous. The Earth view of the chord occultation on Rev 54 is shown in **Fig. 2.2**.

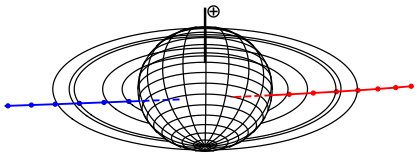

2.1: Rev007

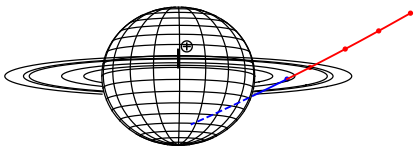

2.2: Rev054

Fig. 2: Earth view of Cassini during the Rev007 and Rev054 ring occultation observations. The red solid lines represent the ingress portion of an occultation and the blue solid lines represent the egress portion. The blue and red dashed lines are the part of the occultation that is blocked by Saturn.

1.4 Cassini RSS ring occultation observations on NASA's PDS

There are two categories of Cassini RSS observations on the PDS: raw data in Radio Science Receiver (RSR) files that contain the digitized spacecraft signal as received at the DSN, and higher-level products (reduced data) that have been processed by the RSS team, including diffraction-reconstructed radial profiles of the optical depth of Saturn's rings and associated geometric and calibration information. `rss_ringoccs` processes raw RSR files and independently produces higher-level products that can be saved as files similar in form and content to those already on the PDS, but with a user-defined radial resolution.

1.4.1 Raw RSS data files

The raw data produced by the DSN that contain the original observations of all Cassini occultation observations are recorded in RSR files, described in more detail in the *Cassini Radio Science Users Guide* (Section 1.5.1). During Cassini RSS occultations, RSR files were typically recorded at two bandwidths: 1 kHz and 16 kHz – both types are available on the PDS for all Cassini RSS ring experiments The `rss_ringoccs` package can handle either version, and they give nearly identical results, although the processing time for the 16 kHz files is significantly longer. We provide convenient scripts in `rss_ringoccs` (Section 2.5) to download both 1 kHz and 16 kHz RSR files before USO failure from the PDS archive.

1.4.2 Higher-level products

Essam Marouf of the Cassini RSS science team has produced a comprehensive set of set of higher-level products for ring occultation observations, available at `https://pds-rings.seti.org/cassini/rss/index.html`. This archive set contains 1- and 10-km resolution diffraction-reconstructed profiles from S-, X- and Ka-band observations of Revs 7 through 137. *Users interested in low-resolution ($\simeq$ 10 km) ring profiles are advised to use the existing PDS results, rather than to use* `rss_ringoccs` *to produce them, since our software package does not implement the low-pass filtering techniques used for the PDS results to obtain the 10 km resolution profiles.*

Using Rev007 as an example, navigate to the dataset CORSS_8001 and then find the data/Rev007/Rev007E/ subdirectory. Occultation data sets are organized here by name: RevXXXev_RSS_YYYY_DOY_B##_D/ (e.g., Rev007E_RSS_2005_123_X43_E/). A description of this naming convention is given below.

- XXX is the rev number (ex: 007)
- ev is the event type (ex: E)

  I for ingress

  E for egress

  CI for ingress portion of a chord occultation

  CE for egress portion of a chord occultation
- YYYY is the UTC year of the start of the occultation (ex: 2005)
- DOY is the UTC day of year of the start of the occultation (ex: 123)
- B indicates the frequency band in which the observations were made (ex: X)
- ## indicates the numeric code for the DSN station from which the observations were made (ex: 43)
- D is the direction (I for ingress, E for egress) (ex: E)

Each occultation data set directory contains a set of *.LBL label files that describe counterpart *.TAB ASCII data tables or a summary PDF file. In addition to the occultation identifiers, all output files are tagged with the date in YYYMMDD on which rss_ringoccs produced the output file as well as a four-digit serial number to distinguish different outputs created on the same date. For example, these are the files output by rss_ringoccs for Rev 7 E observed in X band at DSN station 43 if processed on January 24, 2019:

- Rev007E_RSS_2005_123_ X43_E_SUMMARY_20190124_0001.PDF

  Overview of the occultation
- RSS_2005_123_X43_E_CAL_20190124_0001.{LBL,TAB}

  Calibration information
- RSS_2005_123_X43_E_{FORFIT,FSPFIT}_20190124_0001.PDF

  Fits to frequency offset residual and freespace power
- RSS_2005_123_X43_E_GEO.{LBL,TAB}

  Geometry information.
- RSS_2005_123_X43_E_TAU_0500M_20190124_0001.{LBL,TAB}

  Diffraction reconstructed optical depth profile at 1 km processing resolution
- RSS_2005_123_X43_E_DLP_0100M_20190124_0001.{LBL,TAB}

  Diffraction-limited optical depth profile of the rings sampled at 500 m resolution

rss_ringoccs has the ability to produce CAL, GEO, DLP, and TAU label (LBL) and table (TBL) files that users can compare directly with the higher-order products just described.

1.5 Required and recommended reading

With this overview of RSS ring occultation observations and data in hand, we strongly recommend that all users familiarize themselves with several key documents before using the `rss_ringoccs` package. Our internal documentation of the `rss_ringoccs` code makes frequent reference to the following two documents:

1.5.1 Cassini Radio Science User's Guide

The most complete practical introduction to Cassini RSS ring observations is contained in the *Cassini Radio Science User's Guide*[4] (Asmar et al. 2018). We regard this as *required reading*. Chapter 2 describes the *open-loop* RSR files that contain the raw RSS ring occultation data, and Chapter 3.3 summarizes the analysis steps to produce a diffraction reconstruction ring optical depth profile from the observations. *For the remainder of this guide, we will assume that all readers have familiarized themselves with this material.*

1.5.2 Marouf, Tyler, and Rosen (1986) - MTR86

The definitive reference for diffraction reconstruction of RSS occultations is Marouf et al. 1986: Marouf, Tyler and Rosen's classic "Profiling Saturn's rings by radio occultation." We refer to this as MTR86. For copyright reasons, we cannot include MTR86 in this GitHub repository, but we highly recommend that scientists making use of radio occultation data have this paper readily at hand. It documents the Fresnel inversion method of diffraction reconstruction, complete with application to Voyager RSS occultation observations of Saturn's rings. This is *recommended reading* for beginning users of `rss_ringoccs`, and *required reading* for anyone wishing to understand the inner workings of the `rss_ringoccs` software package.

1.5.3 For more information...

Readers interested in an overview of Cassini RSS instrumentation and science goals are encouraged to read "Cassini Radio Science" by Kliore et al. 2004. Scientific results making use of Cassini RSS occultation observations include Colwell et al. 2009, Moutamid et al. 2016, French et al. 2016a, French et al. 2016b, French et al. 2017 Marouf et al. 2011, Nicholson et al. 2014a, Nicholson et al. 2014b, Rappaport et al. 2009, and Thomson et al. 2007.

2 Setting things up

This section provides step-by-step instructions for setting up the `rss_ringoccs` package and associated data files. We assume that all users are familiar with basic unix commands and introductory-level Python.

2.1 System requirements

The `rss_ringoccs` repository has been developed and tested on the following hardware, unix-based operating systems, and shells:

[4] Available from `https://pds-rings.seti.org/cassini/rss/`

Hardware	Operating System	Shell	GB of RAM
MacBookPro, iMac	MacOS 10.13.4, 10.14.2	csh, bash	8, 16, and 32
Mac mini	Linux Ubuntu Budgie 16	bash	8
MacBookPro	Linux Ubuntu 16	bash	8
ThinkMate	Linux Debian	bash	32

Table 1: Hardware and operating systems

We strongly recommend that users run `rss_ringoccs` on a system with at least 16 GB of RAM (preferably 32 GB) to minimize disk-based memory swapping, which can significantly increase the run time when processing an entire occultation at high resolution.

2.2 Downloading the `rss_ringoccs` repository from GitHub

Follow these steps to download and install `rss_ringoccs`:

- Visit https://github.com/NASA-Planetary-Science/rss_ringoccs and click on the green *Clone or Download* pull-down menu at the upper right.
- Download the zip file `rss_ringoccs-master.zip` to your local `Downloads` directory. For this example, this is `~/Downloads`.
- Identify the destination directory under which you wish to install `rss_ringoccs`. For this example, the destination directory is `~/local`. (This should be on a large-capacity disk drive or partition – 1 TB or larger – since raw Cassini RSS data files are quite large. We recommend that this be routinely backed up.)
- Use your favorite utility to unzip the file. This will create the `rss_ringoccs-master` directory and several sub-directories. For example:

```
cd ~/local
unzip ~/Downloads/rss_ringoccs-master.zip
ls -1F rss*
rss_ringoccs-master:
    LICENSE
    README.md
    ReleaseNotes.md
    data/
    docs/
    examples/
    kernels/
    output/
    pipeline/
    rss_ringoccs/
    rss_ringoccs_config.sh*
    tables/
```

- The current software release of `rss_ringoccs` follows the naming conventions and hierarchy used on the PDS, with some minor changes. Aa brief description of the top-level directories is given on the following page. For a detailed description of the organization of the package, please see the `AAREADME.MD` file contained in the top-level directory of the software release: `rss_ringoccs-master`.

```
|-data/.............. RSR and other raw science data files
|-docs/.............. Documentation
|-examples/.......... Example scripts described in this User Guide
|-kernels/........... Kernel files from NASA/NAIF/SPICE
|-output/............ *.LBL, *.TAB, & plot files produced by rss_ringoccs
|-pipeline/.......... Pipeline scripts for end-to-end and quick-look
                      execution of rss_ringoccs
|-rss_ringoccs/...... Source code
|-tables/............ Reference files tabulating kernel and RSR files
                      available from NAIF and the PDS
```

2.3 Install Python 3 and required packages

`rss_ringoccs` has been developed under Python 3, in particular Python 3.5, 3.6, and 3.7. Our code has been tested under the following Python configurations:

Operating System	Distribution	Version	URL
MacOS 10.14.1	Enthought	3.5.2	https://www.enthought.com
MacOS 10.14.1	Anaconda	3.6.3	https://www.anaconda.com
MacOS 10.14.2	Anaconda	3.7.1	https://www.anaconda.com
Linux Ubuntu Budgie 16	Anaconda	3.6.3	https://www.ubuntu.com
Linux Ubuntu 16	Anaconda	3.6.3	https://www.ubuntu.com
Linux Debian	Anaconda	3.6.3	https://www.debian.org

Table 2: Python versions compatible with `rss_ringoccs`

Once the `rss_ringoccs` package has been downloaded, the user will need to install Python 3 and various dependencies. The easiest way to do this by running the setup script `rss_ringoccs_config.sh`, included in the download. This will install Python 3 using Anaconda, as well as all of the necessary packages. For users who have already installed Python, this script will update conda and then check that Spiceypy and other packages exist on the machine. The script is written in bash, and updates and sources the users .bash_profile. As such, those who use csh or other shell environments will not be able to benefit from this script. If the script does not have executable permissions, the user can change that by using the `chmod` Unix command. An example of running this script is given below.

```
cd ~/local/rss_ringoccs-master/
chmod +x rss_ringoccs_config.sh
./rss_ringoccs_config.sh
```

The installation process will begin, and may take several minutes. This script has been tested for MacOSX 10.13 and 10.14, as well as on Debian and Ubuntu 16. If, for any reason, the script fails, please raise an issue at the following URL: https://github.com/NASA-Planetary-Science/rss_ringoccs/issues. The user may check whether or not the installation was successful by running the script a second time. The following messages should print if the script executed correctly:

```
./rss_ringoccs_config.sh
Running rss_ringoccs_config Script:
    You already have Anaconda on your computer.
    Running updates...
    Checking your PATH variable...
    PATH variable is set
    Sourcing .bash_profile
    Make sure you are using Bash when running rss_ringoccs
Solving environment: done

# All requested packages already installed.

Solving environment: done

# All requested packages already installed.
```

The user may also manually install Python 3 and the required packages by visiting the URLs found in Table 2. A manual installation of either Anaconda3 or Enthought Canopy will provide one with all dependencies, with the exception of the `spiceypy` package.

2.3.1 Download and install `spiceypy`

`rss_ringoccs` makes extensive use of JPL's NAIF SPICE toolkit (Acton 1996), a set of software tools to calculate planetary and spacecraft positions, ring occultation geometry, and a host of useful calendar functions.[5] Our software requires `spiceypy`, a Python-based interface to the NAIF toolkit, available from https://github.com/AndrewAnnex/SpiceyPy. The setup bash script detailed before should setup and install `spiceypy` without any user interaction. If the user decided to manually install Python 3, a manual installation of `spiceypy` will also be needed. Follow the installation instructions on this website, or use `pip`. If you do no already have `pip` on your machine, run the first two lines of the following commands. The third line will install `spiceypy`:

```
curl https://bootstrap.pypa.io/get-pip.py -o get-pip.py
python get-pip.py
pip install spiceypy
```

2.3.2 Test `spiceypy`

To test your installation of `spiceypy`, fire up Python in a terminal at the unix command line and at the `>>>` prompts, enter the following commands to confirm that `spiceypy` returns π and the speed of light c:

```
python
>>> import spiceypy
>>> print(spiceypy.pi(),spiceypy.clight())
3.141592653589793 299792.458
>>> exit()
```

[5] See https://naif.jpl.nasa.gov/naif/index.html

2.4 Download the required JPL/NAIF SPICE kernels

The `rss_ringoccs` package makes extensive use of SPICE data (*kernel* files) from JPL/-NAIF that specify planetary and spacecraft ephemerides, planetary constants, and other essential information for computing the geometric circumstances of occultations.[6] The `rss_ringoccs` distribution contains bash-based shell scripts to automate the retrieval of SPICE kernels from the NAIF website and store them in subdirectories under `rss_ringoccs/kernels/`, following the same directory structure as on the NAIF ftp site. Some of the kernel files are quite large, and will take some time (and significant disk space) to download. The size of the total set of kernel files is 897 Mb, so be sure that there is sufficient disk space available. For quick setup and testing (Section 3.3) purposes, a minimal set of essential kernels is required. To download these, navigate to the directory containing the `rss_ringoccs-master` directory and enter the following commands at the command line of a terminal window:

```
cd ~/local/rss_ringoccs-master/pipeline
./get_kernels.sh ../examples/Rev007_list_of_kernels.txt ../kernels/
cd ../kernels
ls -lR
```

You should have a listing that resembles the following:

```
AAREADME_kernels.txt
naif
./naif:
CASSINI
generic_kernels
./naif/CASSINI:
kernels
./naif/CASSINI/kernels:
lsk
pck
spk
./naif/CASSINI/kernels/lsk:
naif0012.tls
./naif/CASSINI/kernels/pck:
cpck26Feb2009.tpc
earth_000101_180919_180629.bpc
./naif/CASSINI/kernels/spk:
050606R_SCPSE_05114_05132.bsp
./naif/generic_kernels:
spk
./naif/generic_kernels/spk:
planets
stations
./naif/generic_kernels/spk/planets:
de430.bsp
./naif/generic_kernels/spk/stations:
earthstns_itrf93_050714.bsp
```

Notice that there are several Cassini-specific kernel files. Among them are the so-called *reconstructed trajectory* files. For example, `050606R_SCPSE_05114_05132.bsp` is a recon-

[6] For detailed information about kernels, visit https://naif.jpl.nasa.gov/naif/data.html

structed Cassini trajectory file produced on 2005 June 6 (`050606`) that spans the period 2005 day of year 114 to 132 (`05114` to `05132`), or April 24 to May 12, 2005. This reconstructed trajectory file is specific to each rev and should be specified in the meta-kernel.

In order to compute the geometry of RSS occultations throughout the Cassini orbital tour, a larger set of these large trajectory files is required. Once you have completed the initial tests of `rss_ringoccs`, we recommend that you take the time to download this more complete set of files, using the commands below:

```
cd rss_ringoccs-master/pipeline
./get_kernels.sh ../tables/list_of_kernels.txt ../kernels/
```

The shell script detects whether a given kernel has already been downloaded, so you may interrupt this command if it hasn't run to completion in the time you have available, and repeat the command later, picking up the downloading process where it left off the previous time. (NOTE: if you stop the `get_kernels.sh` script while it is downloading a file, the file may be incomplete but will still be detected by future runs of the shell scripts as having been downloaded. You will need to delete incomplete files to restart the download. To check for incomplete files, look in the `lsk`, `pck`, and `spk` directories within the `rss_ringoccs-master/kernels/naif/CASSINI/kernels/` directory and in the `rss_ringoccs-master/kernels/naif/generic/kernels/` directory. The most likely incomplete files will be `.bsp` files located in the `spk/` directory where kernel files for each occultation set of spacecraft and planetary ephemerides are stored; however, it is best to check all kernel directories.) Once you have downloaded the complete set of kernels, you will not need to repeat this process unless JPL releases an updated set of Cassini trajectory files. We plan to update this documentation and the input files for `get_kernels.sh` if that occurs. The meta-kernel for the total set of Cassini and Saturn kernels is located in `../tables/e2e_kernels.ker`, which the user will need to reference when running `rss_ringoccs`.

2.5 Download essential Cassini RSS raw data files

The `rss_ringoccs` package requires local access to raw Cassini RSS data files (Section 1.4.1). The storage capacity on GitHub is not sufficient to allow even one sample RSR file to be part of the standard download. Instead, as with the kernels files described above, we provide a script to download a minimal set of RSR files for the initial tests of `rss_ringoccs`.

```
cd rss_ringoccs-master/pipeline
./get_rsr_files.sh ../examples/Rev007_list_of_rsr_files.txt ../data/
cd ../data
ls -lR
AAREADME_data.txt
co-s-rss-1-sroc1-v10/
    cors_0727/
        SROC1_123/
            RSR/
                S10SROE2005123_0740NNNX43RD.2A1
                S10SROE2005123_0740NNNX43RD.LBL
```

The deeply-nested directory structure of the downloaded data follows that of the PDS website from which the RSR files are retrieved so that users can determine the original source of each RSR file. (Note that only a subset of the RSS files on the PDS is downloaded; the complete PDS distribution contains many additional files that are not needed by `rss_ringoccs`.)

The example 1 kHz RSR file is found under the `co-s-rss-sroc1-v10/` directory - the name indicates that this contains Cassini Orbiter data at Saturn from the RSS instrument (`co-s-rss`) for a Saturn ring occultation (`sroc`). The next level directory `cors_0727/` refers to the Cassini Orbiter Radio Science PDS delivery `0727`. Underneath these directories are directories with names such as `SROC1_123`, which somewhat cryptically refers to a Saturn ring occultation (`SROC`) on day of year 123 of the year during which the data were taken. The RSR files of interest are located in next level `RSR` subdirectories. A typical name is `S10SROE2005123_0740NNNX43RD.2A1`. Decoded, this occultation was part of Cassini sequence 10, it was part of a Saturn ring occultation (`SRO`) – egress (`E`) – in year 2005, day of year 123, beginning at UTC 07:40, recorded at X band (`X`) from Deep Space Network (DSN) station DSS-43. The `r` in `RD.2A1` refers to *right hand circular polarization*, appropriate for all RSS ring occultation observations used by `rss_ringoccs`. The last digit `1` refers to a 1 kHz file, while `2` refers to a 16 kHz file.[7]

To download the full set of pre-USO failure 1 kHz files used in the archived `CORSS_8001` reconstructed data products, use the same command as the example above but replace `../examples/Rev007_list_of_rsr_files.txt` with the list in the `../tables/` directory: `../tables/list_of_rsr_files_before_USO_failure_to_dl.txt`. This will take quite some time to execute, given the large volume (10 GB) of data to be transferred over the internet. Note that the following eight files on the PDS differ in name from the files used in `CORSS_8001`:

`CORSS_8001` file	PDS file
S10EAOE2005_123_0740NNNK34D.1B1	S10SROE2005123_0740NNNK34RD.1B1
S10EAOE2005_123_0740NNNS43D.2B1	S10SROE2005123_0740NNNS43RD.2B1
S10EAOE2005_123_0740NNNX34D.1A1	S10SROE2005123_0740NNNX34RD.1A1
S10EAOE2005_123_0740NNNX43D.2A1	S10SROE2005123_0740NNNX43RD.2A1
S10EAOC2005_123_0229NNNS43D.2B1	S10SROI2005123_0230NNNS43RD.2B1
S12SROE2005177_2226NNNX14RD.2A1	S12SROE2005177_2225NNNX14RD.2A1
S12SROI2005177_1745NNNS14RD.2B1	S12SROI2005177_1740NNNS14RD.2B1
S12SROI2005177_1745NNNX14RD.2A1	S12SROI2005177_1740NNNX14RD.2A1

Table 3: PDS RSR file name changes

In addition, there are three 1 kHz files used by `CORSS_8001` that are currently not available on the PDS. In `../tables/list_of_rsr_files_before_USO_failure_to_dl.txt`, we replace these missing files with their 16 kHz equivalents, shown in Table 4.

[7]For Detailed Documentation, see:
https://pds.jpl.nasa.gov/ds-view/pds/viewProfile.jsp?dsid=CO-S-RSS-1-SROC1-V1.0

1 kHz missing from PDS	16 kHz version
S10EAOI2005_123_0230NNNK26D.3B1	s10sroi2005123_0230nnnk26rd.3b2
S10EAOI2005_123_0230NNNX26D.3A1	s10sroi2005123_0230nnnx26rd.3a2
S10EAOC2005_123_0229NNNX43D.2A1	s10sroi2005123_0230nnnx43rd.2a1

Table 4: Left: 1 kHz files processed in `CORSS_8001` that are currently unavailable on the PDS. Right: 16 kHz equivalent of the missing files. Names are case-sensitive.

`rss_ringoccs` is currently able to process all but two of the files listed in the set of pre-USO failure files, `S43SROI2008239_1410NNNS63RD.1B1` and `S43SROI2008239_1410NNNX63RD.1A1`. The header of each of these files contains `NaN`s for the polynomial coefficients necessary for predicting the frequency offset based on Cassini telemetry at the time of observation, which prevents the pipeline from correctly fitting for the frequency offset (see Section 4.3.1). These files are skipped when running `e2e_batch.py` (in Section 3.5).

2.6 Hard Drive Space

As a part of the hardware requirements for using `rss_ringoccs`, we describe here the requisite hard drive space for running the software. Although the software itself is relatively small in size ($\lessapprox$ 5 Mb), the files needed to produce science data products require a substantial amount of drive space. The full set of kernel files downloaded following Section 2.4 is 897 Mb in size. The full set of 1 kHz RSR files downloaded following Section 2.5 is 10.43 Gb in size. In total, the files required for all occultations observed before USO failure will require 11.35 Gb of drive space.

While this accounts for the initial space necessary for processing every pre-USO-failure occultation observation, the output files for each end-to-end pipeline data reduction will take up additional drive space. A single occultation (e.g., Rev 007 E X43) processed at 0.25 km DLP resolution and 1 km reconstruction resolution will have $\approx$ 520 Mb of output files. The output files containing the DLP and reconstructed profiles (the DLP and TAU files, respectively) are 61.2 Mb each when the profile covers the entire ring system, and these two output file types compose $> 90\%$ of the output file data volume. Because the DLP and TAU files are by far the largest, a smaller radial spacing / higher radial resolution will increase the output file size.

The duration of each occultation observation varies from rev to rev, often depending on the occultation geometry and the elevation angle of Saturn relative to Earth's horizon at any given DSN station. Additionally, the number of bands and DSN stations at which a given occultation is observed also vary. As such, any given RSR file may not yield a complete radial profile resulting in smaller DLP and TAU files. Processing all 154 RSR files prior to USO failure (Section 3.5) will result in 22.66 GB of output files.

2.7 Install A LaTeX Compiler

To make full use of `rss_ringoccs`, you'll need a LaTeX compiler to create the summary PDF files that accompany any given data set. We strongly recommend pdflatex, as this is the only compiler that `rss_ringoccs` has been tested on. MacTeX contains all of the

necessary packages and more, and is recommended for user's of MacOSX who wish to use LaTeX to its full capacity. A download can be found from https://www.tug.org/mactex/mactex-download.html. However, this is a very large download (A few Gigagbytes). To those who only want the necessary compiler and associated binary files, Basictex will suffice. This can be downloaded from https://www.tug.org/mactex/morepackages.html. For linux user's, enter one of the following commands:

```
sudo apt-get install texlive-full
```

or:

```
sudo apt-get install texlive-latex-base
```

This will again download either a plethora of packages for latex and the necessary compiler, or simply the basic necessities. In an attempt to keep the LaTeX portion of the code simple, very few packages are used. A complete list, and how they appear in the code, is given as follows:

```
%----------------------Begin LaTeX Code----------------------%
\usepackage{geometry}
\geometry{a4paper, margin = 1.0in}
\usepackage{graphicx, float}
\usepackage{lscape}
\usepackage[english]{babel}
\usepackage[dvipsnames]{xcolor}
\usepackage[font={normalsize}, labelsep=colon]{caption}
```

In the event of a successful install of either package, all of these dependencies should now be available to the user. Should any error arise, a manual install can be done by visiting the CTAN website. For example, the `float` package can be found from https://ctan.org/pkg/float.

3 Using `rss_ringoccs`

We provide an overview for using `rss_ringoccs`, including requisite information for writing your own scripts to process the data as well as directions to running example scripts.

3.1 End-to-end pipeline outline

As a brief overview, an end-to-end script will require instantiating five separate Python classes in succession:

1. `rsr_inst = rss.RSRReader('RSR_filename.a2a')`
    - Creates an instance of the `RSRReader` class and stores it in `rsr_inst`.
2. `geo_inst = rss.occgeo.Geometry(rsr_inst, 'planet', 'spacecraft', kernels)`
    - Creates an instance of the `Geometry` class and stores it in `geo_inst`.
    - Takes an `RSRReader` instance and user-specified planet, spacecraft, and kernel files.
    - Calculates, among other things, the radial intercept point ρ where the Cassini spacecraft radio signal is occulted by the rings and the locations of gaps in the occultation profile.

- Produces `GEO*.TAB` and `GEO*.LBL` files.
- These and all subsequent output files are written to a user-specified output directory

3. `cal_inst = rss.calibration.Calibration(rsr_inst, geo_inst)`

   - Creates an instance of the `Calibration` class and stores it in the variable `cal_inst`
   - Takes the `RSRReader (rsr_inst)` and `Geometry (geo_inst)` instances
   - This instance contains the calibrations necessary to convert the raw data into a diffraction-limited radial ring profile
   - Calculates the observed frequency of the spacecraft signal to correct the real and imaginary components of the transmittance (I and Q), then estimates the intrinsic received power over the entire occultation
   - Produces `CAL*.TAB` and `CAL*.LBL` files following the naming convention for the GEO files
   - Produces frequency offset residual fit plots (`*FORFIT.PDF`) and free space power fit plots (`*FSPFIT.PDF`)

4. `dlp_inst = rss.calibration.DiffractionLimitedProfile(`

   `rsr_inst, dr, geo_inst, cal_inst`)

   - Creates an instance of the `DiffractionLimitedProfile` class and stores it in the variable `dlp_inst`.
   - Takes the `RSRReader`, `Geometry`, and `Calibration` instances.
   - Contains as attributes the DLP as calibrated and reduced by the previous classes
   - Optional input of radial sampling rate `dr_km_desired` in kilometers
   - Calculates the normalized power P/P_0 and the diffraction-limited optical depth profile assuming $\tau = -\sin B \ln(P/P_0)$
   - Produces `DLP*.TAB` and `DLP*.LBL` files with the same naming convention as the GEO and CAL files with the additional `RRRR` indicator.

5. `tau_inst = rss.diffrec.DiffractionCorrection( dlp_inst,res_km)`

   - Creates an instance of the `DiffractionCorrection` class and stores it in the variable `tau_inst`
   - takes the `DiffractionLimitedProfile` instance and a user-specified reconstruction resolution `res_km` in kilometers
   - Calculates the optical depth profile with reconstruction by accounting for diffraction effects by means of Fresnel inversion at the user specified reconstruction resolution.
   - Produces `TAU*.TAB` and `TAU*.LBL` files following the same naming convention as the DLP files except that `RRRR` here indicates the reconstruction resolution selected by the user when instantiating the `DiffractionCorrection()` class

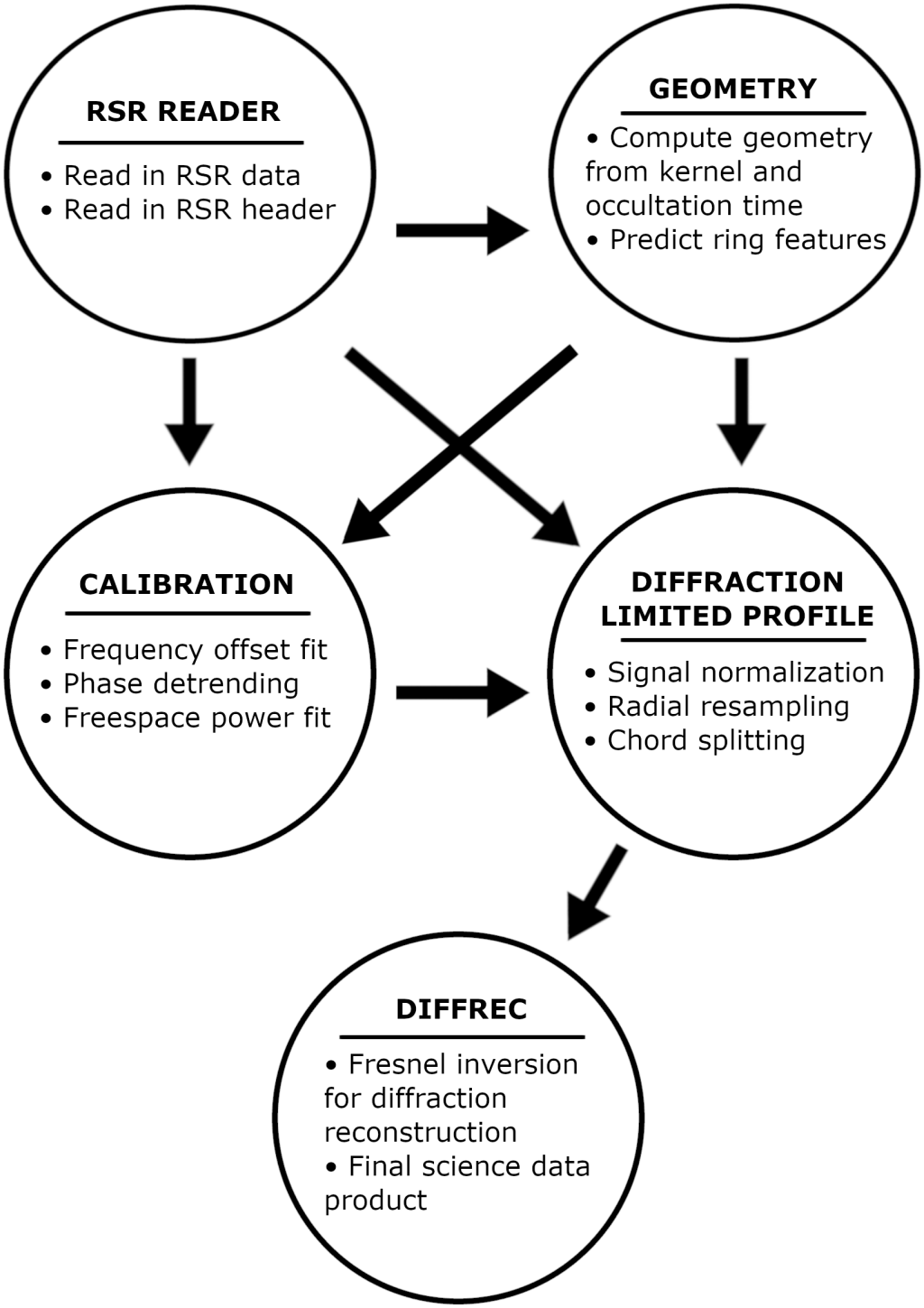

Fig. 3: Data processing pipeline. Each bubble is a separate object called by the `e2e*.py` scripts.

3.2 Conventions and hierarchy

Here, we list some conventions used in the `rss_ringoccs` directory structure/hierarchy and the names of directories and output files.

- No reference is made within the `rss_ringoccs` package to local directories outside of the top-level `rss_ringoccs-master/` hierarchy of directories.

- The directory structure under `rss_ringoccs-master/` *must* strictly follow that of the original download from the GitHub repository.
- For portability, all references within `rss_ringoccs` software to pathnames to other directories within `rss_ringoccs-master/` are relative, not absolute.
- Unless otherwise noted, all executable scripts and Python programs *must* be run from within the `rss_ringoccs-master/pipeline/` directory. (This is so that relative pathnames will point to the correct directories.)
- Output file names follow the format:
  `RSS_OBSY_DOY_B##_D_INF_RRRRRM_YYYYMMDD_XXXX.EXT`
  - `OBSY` is the year the observation was made
  - `DOY` is the day of the year the observation was made
  - `B` is the wavelength band of the observation
  - `##` is the DSN station number
  - `D` is the direction of the occultation
  - `INF` is a three-letter reference specifying the information stored within the file (`GEO` for the occultation geometry, `FOF` for the frequency offset, `CAL` for calibration, `DLP` for the DLP, and `TAU` for the diffraction-reconstructed optical depth profile)
  - `YYYYMMDD` is the year, month, and date on which the user ran the `rss_ringoccs` code
  - `XXXX` is the $XXXX$th run of `rss_ringoccs` on that date
  - `EXT` is the file extension
  - Only DLP and TAU files contain the `RRRRR` in the nomenclature. For the DLP files, `RRRRR` is the minimum reconstruction resolution (the so-called "DLP resolution" in MRT86) in meters while for TAU files this is the processing resolution selected by the user
  - The output LBL files match those from the PDS with minor changes.

With these caveats in mind, users are highly encouraged to write their own scripts to call upon and make full use of the `rss_ringoccs` package. To that end, we provide example scripts for both pipeline versions as well as specific portions of the pipeline.

3.3 End-to-end pipeline: A look at the Huygens ringlet

The "end-to-end" pipeline process is a set of steps that need to be performed only once when processing a given RSR file from scratch. For the initial run, users will need to supply an RSR file, a set of kernels to use, a radial spacing to resample to, and a reconstruction resolution (there are also default keyword inputs documented within each routine). The RSR extraction, geometry calculation, and frequency offset calculation steps are all automated; however, users may specify several options and parameters in advance by editing the input file `e2e_run_args.py` in the `./examples/` directory. These options include whether to process 16 kHz files, whether to write results to output files, whether to output to terminal, and whether the pipeline should enter an interactive

mode to customize the freespace power fitting. This interactive mode will display the automated fit results in a `matplotlib` plotting window and prompt the user for changes to the fit parameters and/or freespace regions.

At the end of the end-to-end run, if the write_file keyword argument is set to True, several data files will be generated: geometry files, calibration files, diffraction-limited profile files, reconstructed optical depth files, and a summary file. Each class instantiated in the end-to-end pipeline process corresponds to a specific set of output files which match those on the PDS. Once these files have been produced, users can use the quick-look process for subsequent runs.

Also included in the pipeline's arguments file are various and sundry parameters for customizing the calibration steps and the profile ranges and resolutions. Detailed discussion of which resolution values to choose and definitions of each type of resolution are given below.

As a demonstration of this end-to-end pipeline, we provide an example script which runs through the entire pipeline and examines the Huygens ringlet. To execute this script, follow the example below.

```
cd rss_ringoccs-master/examples
python e2e_run.py
```

This will automatically produce a plot identical to Fig. 4. The top row of plots show the raw power, optical depth, and phase profiles that were input to `DiffractionCorrection`, and the bottom row shows the Fresnel-inverted output.

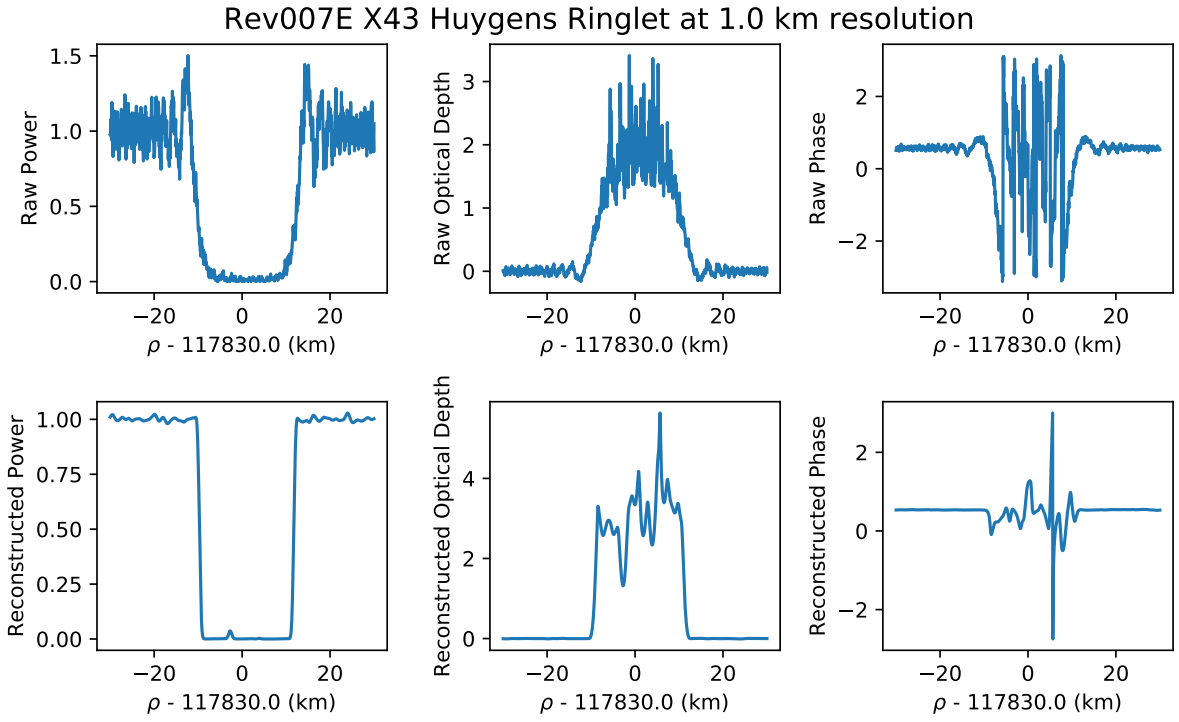

Fig. 4: Power, optical depth, and phase plots produced by e2e_run.py

3.4 Quick-look method: Comparing profiles reconstructed at different resolutions

The quick-look approach allows users to save computation time by utilizing pre-computed data files. For these runs, users start directly at the Fresnel inversion step of the pipeline, provided they have a set of `GEO*.TAB`, `CAL*.TAB`, and `DLP*.TAB` files. Users must specify the relative file path(s) and desired `*.TAB` files to the `tools.ExtractCSVData()` class to create a DLP instance like the one instantiated in the end-to-end pipeline from the `calibration.DiffractionLimitedProfile()` class. This DLP instance can then be passed to the `diffrec.DiffractionCorrection()` class.

Continuing with the RSR file downloaded in Section 2.5, we provide an example script to demonstrate diffraction-reconstructed optical depth profiles at different reconstruction resolutions for the Maxwell Ringlet. Before running, users will need to open the script in a text editor and change the `*_file` variables to include the appropriate file names as a string after the pre-specified path. For the first set of Rev007 files output by the `e2e_run.py` script, this might resemble

```
dir = '../output/Rev007/Rev007E/Rev007E_RSS_2005_123_X43_E/'
geo_file = dir+'RSS_2005_123_X43_E_GEO_20180926_0001.TAB'
cal_file = dir+'RSS_2005_123_X43_E_CAL_20180926_0001.TAB'
dlp_file = dir+'RSS_2005_123_X43_E_DLP_0100M_20180926_0001.TAB'
```

To execute the example quick-look script, follow the example below

```
cd rss_ringoccs-master/examples
python quick_look_run.py
```

This will produce optical depth profiles at four different reconstruction resolutions: 1 km, 0.75 km, 0.5 km, and 0.25 km for the Rev007 egress X band observation processed by the end-to-end script in Section 3.3. Running the script will produce the plot in Fig. 5 (not including the reference red line for PDS data).

3.5 Batch Scripts

To simplify and expedite the use of `rss_ringoccs` to process large numbers of files, we provide a single python script `e2e_batch.py` in `./pipeline/` which, when executed, will run the end-to-end pipeline for a list of files referenced in a reference ASCII text file. The default list, `list_of_rsr_files_before_USO_failure_to_dl.txt`, is the same list of files used by `get_rsr_files.sh` to download all of the 1 kHz Cassini RSR files prior to the USO failure, and can be found in the `tables/` directory. This batch script, like the single-file script, reads in a file of parameters, `e2e_batch_args.py`, which specifies, among other things, radial sampling rates, calibration fit orders, profile range, and whether to output files. By modifying the contents of `e2e_batch_args.py`, users can produce on-demand, customized optical depth profiles for specific data sets and radial regions of interest. Each option within `e2e_batch_args.py` is documented in comments. For more information, we refer users to either §4 or the documentation online at https:\rss-ringoccs.readthedocs.io.

The default end-to-end pipeline will jump into its interactive mode when the normalization of the received power to a nominal free-space level is poor. To avoid this interactive

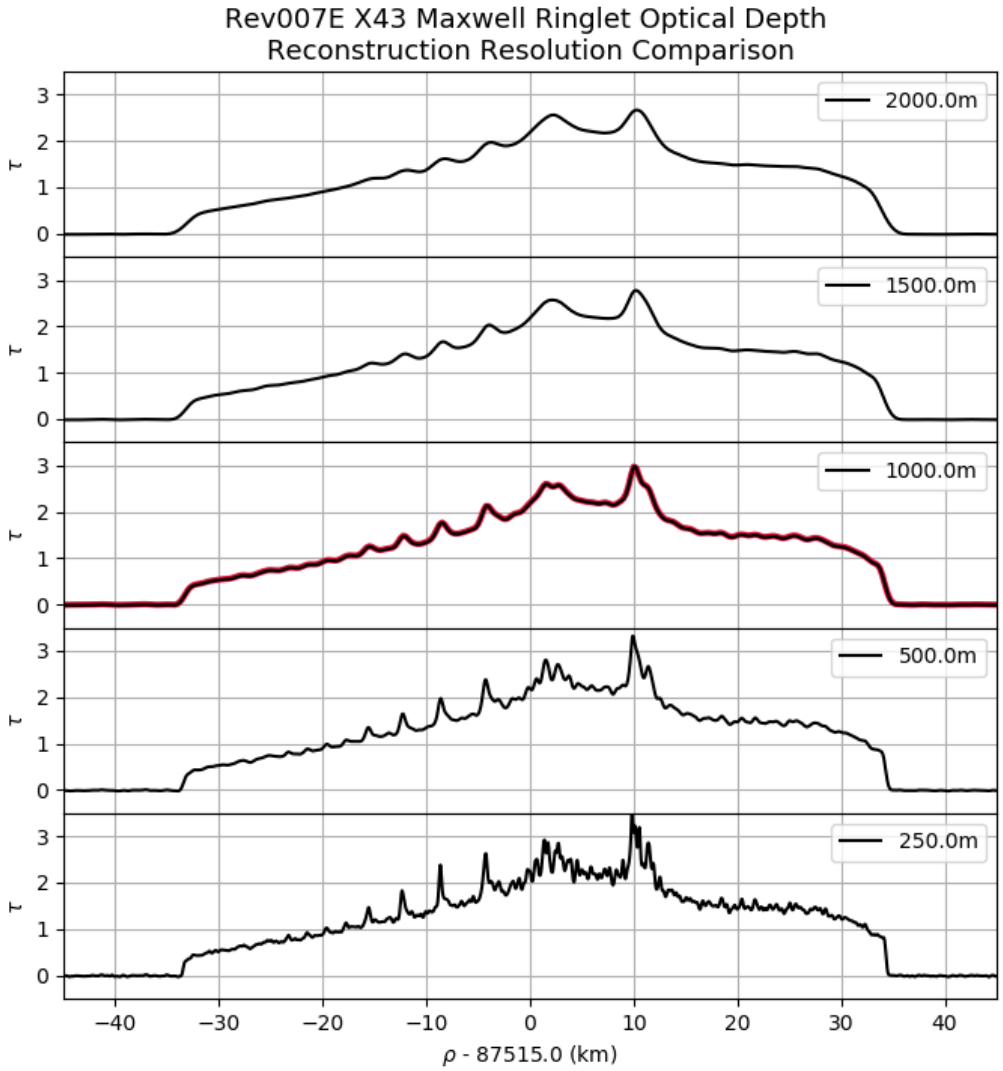

Fig. 5: Optical depth profile for the Maxwell ringlet from the Rev007E X43 occultation reconstructed at 2 km, 1 km, 0.5 km, and 0.25 km resolution. Solid black lines are the optical depth profile produced by the quick-look example script at various processing resolutions indicated by the plot text. For reference and validation, the solid red line is the 1 km reconstruction resolution profile obtained from the PDS3.

mode, one can alternatively run the script using the `yes` command to automatically enter the string "yes" for all input prompts (thus accepting the default fit, should `rss_ringoccs` enter interactive mode) and the `tee` command to store any and all information output by the command line to a reference file. Running the batch script in this manner will resemble

```
yes | python e2e_batch.py | tee ../output/e2e_batch_yyyymmdd.out
```

(You should replace `yyyymmdd` with the date of the run.) In addition to the `tee` file, a `e2e_batch.err` file will automatically be generated. We recommend that users write-protect both `e2e_batch.err` and `e2e_batch_yyyymmdd.out` so that neither file gets over-written by subsequent runs. This can be done by typing the following in the terminal after the batch has finished:

```
chmod -w ../output/e2e_batch_yyyymmdd.out
chmod -w ../output/e2e_batch.err
```

The `.err` file will contain names of files that failed to process during the batch run as well as the resulting traceback error. `rss_ringoccs` is known to currently fail for just two RSR files, Rev082 S63 and X63, so these are intentionally skipped. If `verbose` keyword argument is set to `True`, some benign messages, such as:

```
1) WARNING (RSRReader): file size not the same as expected!
2) DETECTED INGRESS (resample_IQ.py): reversing arrays
```

will be printed to the terminal. These do not result in failed processing runs and are therefore not printed to the `.err` file.

One of these default parameters is `with16=False`, which skips 16 kHz files that have no corresponding 1 kHz files (see §2.5, Table 4). Only set this to `True` if the user's computer has at least 16 Gb RAM; these files will also take about 10-15 times longer to process than a typical 1 kHz file.

3.6 Profile Resolution

As a practical matter, most users would like to know: "What is the highest achievable resolution for a given ring occultation, and how can I use `rss_ringoccs` to produce a radial profile at that resolution?" The answer is complicated by a variety of definitions of resolution – we clarify these below – and is also affected of course by the SNR of any given occultation, which depends on the wavelength of the observation, the observing conditions at the DSN, the size of the receiving antenna, the geometry and speed of the occultation, and host of other factors.

Our recommendation is that users begin with the 1-km reconstructions available on the PDS, to get a sense for the signal quality of a specific occultation of interest. As a next step, we provide an end-to-end script that uses `rss_ringoccs` to process the entire set of Cassini RSS occultation data (up to the point of the USO failure) at a diffraction-corrected resolution of 0.5 km. Users can compare these profiles with the 1.0 km results available on the PDS, and decide whether reconstruction at a different resolution is needed.

In cases where higher resolution is desired and is warranted by the SNR, we recommend that `rss_ringoccs` users produce diffraction-reconstructed radial profiles at successively finer resolutions (centered on a feature of interest over a limited radial range to reduce processing time). As the resolution is increased, the effects of noise will eventually limit the useful information that can be obtained for a particular science goal.

To carry this out in practice, it is important to understand the factors that affect the diffraction-reconstructed resolution. Prior to diffraction reconstruction, RSS observations are limited in resolution at a spatial scale comparable to the Fresnel scale $F \approx \sqrt{\lambda D/2}$, where λ is the wavelength of observation and D is the distance between the spacecraft and the ring plane. Geometrical effects such as the tilt of the ring plane result in multiplicative scale factors applied to F, when converted to an effective diffraction-limited resolution in

the radial direction in the ring plane, but as a general rule, the effective Fresnel scale for RSS ring measurements is of order a few km for typical occultations.

The task of diffraction reconstruction is to improve on the diffraction-limited resolution of the observations by making use of both the intensity and phase of the received signal across the diffraction pattern. Intuitively, it makes sense that a high-resolution diffraction reconstruction will require finer resolution of the observed diffraction pattern, over a larger radial range (what we refer to as a *filter window* – see MTR86 for details), than a low-resolution reconstruction. For sub-km diffraction reconstruction at S-band (the longest of the three Cassini wavelengths), the filter window can extend for hundreds of km to either side of the location of the feature of interest, and it must be sampled at a fine enough spatial scale to capture the diffraction fringes produced by the ring feature over the entire filter window.

From these considerations, it's clear that in order to achieve a given post-reconstruction resolution, there is an implied requirement on the resolution at which the diffraction-limited profile is calculated. To satisfy the sampling theorem, if the radial sampling of the diffraction-limited DLP profile is $\Delta\rho$, the subsequent diffraction reconstruction resolution can only have shortest resolvable wavelengths of Nyquist or higher (i.e., $\geq 2\Delta\rho$) – more on this in a moment! As a practical matter, it sometimes makes sense to produce a DLP profile once and for all at very high resolution (say, 0.05 km), use it to produce a diffraction-reconstructed profile at, say, 1 km resolution, and then to reuse this same DLP profile to explore the SNR properties of successively higher resolution diffraction reconstructions, consistent with the sampling theorem.

The original data are a time series sampled at regular intervals in time, but all of our processing is done in terms of ring plane radius. To achieve uniform radial sampling, we take account of the changing velocity and trajectory of the spacecraft and resample the phase-corrected complex signal at a user-defined spacing $\Delta\rho$ (passed to the `DiffractionLimitedProfile` as the positional argument `dr_km` when instantiating the class). We suggest a value for `dr_km` no smaller than 0.05 km.

To satisfy the sampling theorem, the subsequent diffraction reconstruction resolution can only have shortest resolvable wavelengths of Nyquist or higher (i.e., $\geq 2\Delta\rho$). However, the situation is complicated by a variety of definitions of diffraction reconstruction resolution. As MTR86 make clear (see Eqs. 10–14), resolution can be defined in terms of the the filter window width W either as the null-to-null width of the main diffraction lobe, or as the equivalent width of the normalized impulse response profile – these definitions differ by a factor of two from each other. Uncertainty in the Fresnel scale can further degrade the effective resolution, as can limitations on the validity of the approximations made to compute the phase of the signal.

In our development of `rss_ringoccs`, we used the MTR86 Eq. 11 definition of effective resolution $\Delta R_W = 2F^2/W$, using the geometrically scaled definition of F given by MTR86 Eq. 6. This is the definition used throughout MTR86 in the analysis of Voyager RSS data, and it matches our results when we apply diffraction reconstruction to the archived PDS Voyager RSS diffraction-limited profiles. We refer to this as the *processing resolution* ΔR within `rss_ringoccs`.

As it happens, Essam Marouf introduced yet another definition of resolution in his Cassini reconstructed profiles recently submitted to the PDS, based on applying a low-pass filter to the diffraction reconstruction. The relation between ΔR_W and this new PDS definition of resolution is given by

$$\Delta R_W = 0.75 \Delta R_{\rm PDS}$$

or

$$\Delta R_{\rm PDS} = \frac{4}{3} \Delta R_W .$$

Given these two definitions, and a lack of information about the details of the low-pass filter used by Marouf, we faced a choice: should we retain the definition of resolution as derived in MTR86 and apparently used for Voyager RSS results, or should we be consistent with the recent PDS contributions by Marouf? We chose the latter approach, so that our `rss_ringoccs` runs can be directly compared to the PDS results at the same quoted post-reconstruction resolution. The user specifies a desired resolution $\Delta R_{\rm PDS}$ for the reconstructed profile through the `res` positional argument when instantiating the `DiffractionCorrection` class. The resolution specified by `res` is then scaled within this class to the processing resolution ΔR by the factor of 0.75 described above.

In our interpretation of the sampling theorem, `rss_ringoccs` requires that $\Delta R_W > 2\Delta\rho$. In terms of the requested diffraction-corrected resolution $\Delta R_{\rm PDS}$, this places the following restriction on the pre- and post-diffraction reconstructed resolutions:

$$\Delta R_{\rm PDS} > \frac{8}{3} \Delta\rho .$$

The factor of 8/3 is both cumbersome and non-intuitive, but is the best compromise we could find. As specific example, for a DLP file produced at 0.05 km resolution ($\Delta\rho = 0.05$ km), the requested post-diffraction resolution $\Delta R_{\rm PDS}$ (or `res`) must be no smaller than $8/3 \times 0.05 = 0.133$ km. (This is likely to be below the useful resolution of any Cassini RSS ring data.) If the user violates these conditions, an informative error message will be displayed, made more comprehensible (we hope!) by this extensive discussion.

4 A detailed look at `rss_ringoccs`

Here, we elaborate on the inner workings of `rss_ringoccs`, detailing the methods and goals of each step of the software pipeline in order to make this software as accessible and transparent as possible. For documentation and definition of individual variables, functions, methods, and modules, we refer the user to our online reference available at https://rss-ringoccs.readthedocs.io/en/master/.

4.1 RSR reader

The `rsr_reader/` subpackage is used for extracting information from a given RSR file. The `RSRReader` class, when instantiated with a linked RSR file, extracts the raw complex signal I and Q from the RSR file from the PDS as well as some accompanying non-geometric meta-data stored in the RSR file header such as the DSN station, observation dates, sampling rate, start and end times of the observation, and the band of observation.

4.2 Occultation geometry routines

The routines in `occgeo/` depend heavily on the NAIF SPICE Toolkit and are geared towards reproducing all occultation geometry parameters that are documented within `Archived_Cassini_RSS_RingOccs_2018`, or `CORSS_8001 v2`, submission (see Table 5). In addition to these parameters, `Geometry` also calculates the elevation angle of the observation at the DSN station, the optical depth enhancement factor β, and the effective ring opening angle B_{eff}. Using orbital parameters compiled from literature and the computed ring azimuth and ring radius, `Geometry` uses the `find_gaps` method from the `cal_occ_geo` module to determine the locations of gaps in the ring system in the occultation data set. This is done iteratively by repeating the following steps, choosing the semimajor axis of the gap edge for the initial predicted edge radius:

1. Find the ring radius in the occultation data set closest to the predicted gap edge radius.
2. Find the ring azimuth and orbital time implied by the closest ring radius.
3. Predict the radius of the gap edges using compiled orbital properties and the implied ring azimuth and time.

Symbol	Parameter Name	`Geometry` Attribute
t_{OET}	OBSERVED EVENT TIME	t_oet_spm_vals
t_{RET}	RING EVENT TIME	t_ret_spm_vals
t_{SET}	SPACECRAFT EVENT TIME	t_set_spm_vals
ρ	RING RADIUS	rho_km_vals
ϕ_{RL}	RING LONGITUDE	phi_rl_deg_vals
ϕ_{ORA}	OBSERVED RING AZIMUTH	phi_ora_deg_vals
B	OBSERVED RING ELEVATION	B_deg_vals
D	SPACECRAFT TO RING INTERCEPT DISTANCE	D_km_vals
V_{rad}	RING INTERCEPT RADIAL VELOCITY	rho_dot_kms_vals
V_{az}	RING INTERCEPT AZIMUTHAL VELOCITY	phi_rl_dot_kms_vals
F	FRESNEL SCALE	F_km_vals
R_{imp}	IMPACT RADIUS	R_imp_km_vals
r_x	SPACECRAFT POSITION X	rx_km_vals
r_y	SPACECRAFT POSITION Y	ry_km_vals
r_z	SPACECRAFT POSITIION Z	rz_km_vals
v_x	SPACECRAFT VELOCITY X	vx_kms_vals
v_y	SPACECRAFT VELOCITY Y	vy_kms_vals
v_z	SPACECRAFT VELOCITY Z	vz_kms_vals
θ_{EL}	OBSERVED SPACECRAFT ELEVATION	elev_deg_vals

Table 5: Glossary of parameters in *GEO.TAB file in PDS submission `Cassini_RSS_Ring_Profiles_2018_Archive` and their corresponding attribute names within the `Geometry` class.

This iterative process returns the gap edge radius once it converges on a solution (i.e., when the difference between two consecutive radius predictions is less than one meter) which occurs within five iterations or less. The inner and outer edges of each gap are then stored as an attribute of the `Geometry` object instance for future use.

To create an instance of `Geometry`, or `geo_inst`, users will need an instance of the `RSRReader` class (`rsr_inst`), a target planet, a target spacecraft, a set of kernels over the

duration of the RSR file used in `rsr_inst`, and, optionally, a desired number of points per seconds for all calculations (the default is 1 point per second). For choosing an RSR file, which is the only input necessary for instantiating `RSRReader`, see Section 6.2.

4.3 Calibration routines

All of the routines to produce a calibrated diffraction pattern are in the `calibration/` directory in the `rss_ringoccs` package. Each of them performs a portion of the frequency and power calibration steps. Every step of the calibration process is handled by the `Calibration` class. When instantiated (which requires the appropriate instances of the `RSRReader` and `Geometry` classes), it calls the `FreqOffsetFit` class to compute the offset frequency needed for phase-correcting the measured complex signal. Then, the signal is phase-corrected using the `Calibration` class method `correct_IQ` following Marouf et al. (1986) and Asmar et al. (2018). The phase detrending function ψ is computed from the cumulative integral:

$$\psi = \int^{t} \hat{f}(\tau)_{offset}\, \mathrm{d}\tau + \psi(t_0) \tag{1}$$

and used for detrending the complex signal such that:

$$I_c + iQ_c = [I_m + iQ_m] \exp(-i\psi) \tag{2}$$

(Asmar et al. 2018, Equations 17 and 18). Then, `Calibration` normalizes the phase-corrected signal, using the `Normalization` class to estimate the intrinsic spacecraft power $\hat{P}_0$ as it changes over the course of the occultation.[8] Finally, all the results of the calibration are written out to an `LBL` and a `TAB` file following the naming conventions discussed above.

4.3.1 Frequency Offset

To estimate the offset frequency over the entire occultation, we compute the offset frequency $f(t)_{offset}$ directly from the raw data using a series of "rolling-window" FFTs. The predicted frequency is then computed from the Doppler shift implied by spacecraft ephemerides (the so-called *reconstructed* sky frequency $f(t)_{dr}$ computed from spacecraft ephemerides) and the polynomial coefficients provided in the RSR file header (which give $f(t)_{dp}$, the *predicted* sky frequency). Following Asmar et al. (2018), we define the residual offset frequency as:

$$f(t)_{resid} = f(t)_{offset} - (f(t)_{dr} - f(t)_{dp}) \tag{3}$$

and fit this using a polynomial of order `fof_order`, a keyword argument specified by the user when instantiating the `Calibration` class (default is 9). The resulting fit $\hat{f}(t)_{resid}$ allows recovery of values of frequency offset where the value calculated from the data is unreliable (whether noisy or highly extinguish by ring material or the atmosphere). Final offset frequency is given by:

$$\hat{f}(t)_{offset} = \left(f(t)_{dr} - f(t)_{dp}\right) + \hat{f}(t)_{resid} \tag{4}$$

as defined by Equation 19 in Asmar et al. (2018). This is stored as an attribute of the `FreqOffsetFit` class for use by the phase detrending method in the `Calibration` class.

[8] Limits on the reliability of the normalized power are estimated in the form of threshold optical depth, which is computed by the `calc_tau_thres` class when instantiating `DiffractionLimitedProfile()`.

When instantiated, the `FreqOffsetFit` class begins by instancing the `calc_freq_offset` class, which contains methods to calculate the frequency offset as a function of time from the raw data. It uses the time (`spm_vals`) and raw signal $I_m + iQ_m$ (`IQ_m`) attributes of RSRReader class (`rsr_inst`). Its positional arguments are an instance of the RSRReader class (`rsr_inst`) and two floats specifying the minimum and maximum SPM values to use as limits on the range of occultation data for which the offset frequency is computed (this reduces computation time by eliminating the calculation of offset frequencies that are not useful for constraining the offset frequency residuals). Its optional inputs are `dt_freq` for the FFT window size in seconds from which to calculate frequency offset (default is 131.072 seconds; to avoid rounding error, we suggest choosing an FFT window size that is a power of two, which is accurately represented in binary) and `verbose` for a Boolean specifying whether to print out intermediate steps to the terminal (default is `False`).

To calculate frequency offset from the data, we use the `numpy` FFT module to compute the frequency components of the raw measured complex signal for a window in time with a width of `dt_freq`. The submodule `calc_freq_offset` estimates the frequency corresponding to the peak in the power spectrum near the center of the bandwidth by applying a Hamming filter to the signal within the window, computing the FFT, converting the FFT from discrete to continuous, and obtaining the frequency associated with the maximum power ($|A^2|/N$). The result is stored in an array. Then, the window center is shifted forward in SPM by the sampling resolution value, and the process is repeated. The first window is centered at the initial SPM value plus half with window width and are sampled at the keyword-specified resolution until the window center is half a window width from the end of the time series.

Symbol	Parameter Name	`Calibration` Attribute
t_{OET}	OBSERVED EVENT TIME	t_oet_spm_vals
$\hat{f}(t)_{sky}$	SKY FREQUENCY	f_sky_hz_vals
$\hat{f}(t)_{resid}$	RESIDUAL FREQUENCY	f_sky_resid_fit_vals
$\hat{P}_0$	FREESPACE POWER	p_free_vals

Table 6: Glossary of calibration data in the CAL files.

The `FreqOffsetFit` class then calls `calc_f_sky_recon` to compute the reconstructed sky frequency. This uses spacecraft ephemerides available in the kernel files to determine the implied line-of-sight Doppler shift of the intrinsic USO frequency, denoted as $f(t)_{dr}$. Using information stored in the RSR file header, the `RSRReader` method `calc_f_sky_pred` computes the predicted sky frequency of the spacecraft signal, denoted as $f(t)_{dp}$. Together with the offset frequency $f(t)_{offset}$, we calculate the residual difference $f(t)_{resid}$ between the observed and anticipated spacecraft signal frequency using Equation 3.

With its method `create_mask`, `FreqOffsetFit` performs sigma clipping of the residual offset frequency to exclude data which are unreliable by creating a boolean mask array. The method begins by masking out all residual frequencies which more than five standard deviations away from the medial residual frequency. Then, this method fits data with a

ninth-order polynomial and excludes data which are more than five standard deviations away from the initial polynomial fit estimate. In order to exclude spurious inclusion, `create_mask` performs a "nearest-neighbor" comparisons that assumes any datum with at least four excluded nearby data points should also be excluded. Finally, a boolean mask array is returned which ignores all unreliable data.

`FreqOffsetFit` uses its `fit_f_sky_resid` method to fit a polynomial of user-specified order (through the `fof_order` keyword when instantiating the `Calibration` class) to the masked residual frequency offset data using the `numpy.polynomial` subpackage. The best-fit polynomial $\hat{f}(t)_{resid}$ is returned along with the reduced summed squared residuals as an estimate of the fit quality.

Following Eqn. 4, `FreqOffsetFit` computes $\hat{f}(t)_{offset}$ and stores both the $\hat{f}(t)_{resid}$ and $\hat{f}(t)_{offset}$ variables as attributes. For reference and visual assessment, `FreqOffsetFit` plots the total and sigma-clipped sets of $f(t)_{resid}$ and overplots $\hat{f}(t)_{resid}$. The plot is saved in the appropriate output directory and is named following the `*.TAB` and `*.LBL` conventions with the infix `FORFIT`.

4.3.2 Power Normalization

After phase compensation of the complex signal, the `Calibration` class instantiates the `Normalization` class. The objective of this class is to estimate the intrinsic spacecraft signal power $\hat{P}_0$ by fitting the observed power in free space regions with a low-order polynomial. A `Normalization` instance requires $I_c + iQ_c$ and an instance of the `Geometry` class (`geo_inst` in the pipeline scripts).

To begin, `Normalization` down-samples the corrected complex signal by a factor of 500. This serves to minimize the effect diffraction patterns in the free space regions might have on the overall prediction of $\hat{P}_0$ while expediting the fitting procedure.

Next, `Normalization` utilizes the ring gaps and other free space regions predicted by the `find_gaps` function in the `calc_occ_geo` submodule in units of SPM. Free space regions are then excluded or retained by comparing the median power within the SPM limits of the free space region to the maximum power *within* the ring system. Because extinction by the ring material causes a decrease in observed signal power, this effectively select the maximum power observed in gaps and divisions inside of the ring system. When the median power within a given free space region is 50% below or 25% above the maximum ring-system spacecraft signal power, the data from this free space region is excluded. After these comparisons and rejections are made, data from all remaining free space regions are culled for use in a polynomial fit.

Then, the `Normalization` method `fit_freespace_power` fits these reliable measurements of the intrinsic spacecraft signal in order to predict $\hat{P}_0$ over the entire occultation. The default fit is a third order polynomial; however, the fit order can be changed when instantiating the `Calibration` class using the keyword argument `pnf_order` and the fit type can be set using the keyword argument `pnf_fittype` (default of "poly" for polynomial and "spline" for spline, piece-wise is on lien for future versions). Regardless of user input, if the number of free space regions is less than five, the fitting method forces the fit order

to linear.

If the keyword `interact` is set to `True` when instantiating the `Calibration` instance, `Normalization` will enter its interactive mode after computing the best fit to the reliable free space data. In this mode, users can customize the free space regions, fit type, and fit order following prompts in the terminal. The command line will prompt the user to confirm interactive mode and subsequently display a plot in a `matplotlib.pyplot` window showing the best-fit polynomial to the default free space regions. Both the individual regions and the total profile will be displayed so that the user may assess the quality of the fit (in the same manner as the output fit plot, as shown in Figure 13). The command line will then prompt users whether to change included free space regions or revert to the defaults generated by the automated pipeline (see Appendix C for an example). If the user opts to change the free space regions, new definitions for the desired free space regions (specified as pairs of lower and upper SPM limits for each region) will need to be entered in the following format

```
[[30500,31785],[34080,34245],[35285,36000]]
```

to be used in the fit. If the new free space region limits are not entered in the appropriate format, the code will revert to the initial freespace regions predicted by `Geometry`.

Once the final fit has been computed, $\hat{P}_0$ and the boundaries of the free space regions used to compute the fit are stored as attributes. As with the frequency offset residual fit, this step also includes plotting the fit results for visual inspection and reference. $\hat{P}_0$ is plotted over the phase-compensated signal power for both the entire profile and for each individual free space region used in the fit. Naming convention follows that of the `*.TAB` and `*.LBL` files with the infix `FSPFIT`.

4.4 Diffraction-limited profile routines

Symbol	Parameter Name	`NormDiff` Attribute
ρ	RING RADIUS	rho_km_vals
$\Delta\rho_{IP}$	RADIUS CORRECTION DUE TO IMPROVED POLE	rho_corr_pole_km_vals
$\Delta\rho_{TO}$	RADIUS CORRECTION DUE TO TIMING OFFSET	rho_corr_timing_km_vals
ϕ_{RL}	RING LONGITUDE	phi_rl_rad_vals
ϕ_{ORA}	OBSERVED RING AZIMUTH	phi_ora_rad_vals
τ	NORMAL OPTICAL DEPTH	tau_norm_vals
ϕ	PHASE SHIFT	phase_rad_vals
τ_{TH}	NORMAL OPTICAL DEPTH THRESHOLD	tau_threshold_vals
t_{OET}	OBSERVED EVENT TIME	t_oet_spm_vals
t_{RET}	RING EVENT TIME	t_ret_spm_vals
t_{SET}	SPACECRAFT EVENT TIME	t_set_spm_vals
B	OBSERVED RING ELEVATION	B_rad_vals

Table 7: Glossary of optical depth, phase shift, and selected geometry parameters contained in the DLP files.

When instantiated, the `DiffractionLimitedProfile` class normalizes the power profile using the results from the `Calibration` step and resamples it with respect to uniformly-spaced ring radius at a sample spacing $\Delta\rho$. The `DiffractionLimitedProfile` class

requires all previous class instances as arguments: the `RSRReader` class (`rsr_inst`), the `Geometry` class (`geo_inst`), and the `Calibration` class (`cal_inst`). The final positional argument `dr_km` specifies the radial sample spacing of the profile. Keyword arguments consist of the `verbose` – a boolean specifying verbose mode (default is `False`), `write_file` – a boolean specifying whether to write the DLP out to a CSV file (default is `True`), and `profile_range` – a 1×2 list setting the lower and upper limits of the DLP (default is `[65000,150000]`; we highly recommended users proceed with these default limits).

When instantiated, the `DiffractionLimitedProfile` calls the `resample_IQ` module to resample the phase-detrended signal $I_c + iQ_c$ with respect to ring radius over the range `profile_range` at radial spacing of `dr_km`. From the resampled detrended complex signal, `DiffractionLimitedProfile` computes the phase

$$\phi_c = \arctan(Q_c/I_c) \tag{5}$$

and normalized complex signal

$$\hat{T} = \hat{T}_R + i\hat{T}_I = (I_c + iQ_c)/\hat{P}_0, \tag{6}$$

the latter following from Equation 2 in Marouf et al. (1986) and Equation 20 in Asmar et al. (2018). It is from $\hat{T}$ that the DLP normal optical depth τ_{DLP} is calculated by:

$$\tau_{DLP} = -\sin(|B|)\ln(\hat{T}) \tag{7}$$

Finally, `DiffractionLimitedProfile` calls the `calc_tau_thresh` submodule to compute the threshold optical depth τ_{TH}, a proxy for the maximum reliable value of τ_{DLP}.

For the DLP instance to be of use in the subsequent diffraction reconstruction step of the pipeline, $\dot{\rho}$ can only have one sign. Chord and proximal orbit occultations thus present a problem if not handled appropriately when creating the DLP object.
`DiffractionLimitedProfile` handles this issue by using a class method to return an object instance of itself for each direction of the occultation as indicated by the sign of $\dot{\rho}$. For the user, this means that instantiating the `DiffractionLimitedProfile` object class will always return two objects: one for ingress and one for egress (always in this order). For diametric occultations, the object corresponding to the direction *not* included in the observation will be a `None` object in place of a DLP instance. For chord occultations, the user will receive two DLP object instances, one for ingress and one for egress, split where a sign change in $\dot{\rho}$ occurs. Each DLP object can be passed individually to the diffraction reconstruction step in the pipeline.

4.4.1 Threshold Optical Depth

The threshold optical depth is an estimate of the maximum reliable value of optical depth implied by the signal-to-noise ratio SNR_0. The noise is estimated from the spectrogram of the entire observation of raw $I + iQ$. After computing the spectrogram, we average the power spectrum over the frequency ranges -450 to -200 Hz and 200 to 450 Hz so as to eliminate both the spacecraft signal and the rolloff at the edges of the power spectrum. Then, we average the frequency-averaged power over the first and last thousand seconds of the observation to exclude possible contamination from scattered spacecraft signal while maintaining a large number of samples of the noise. The intrinsic signal $\hat{P}_0$ is assumed

to be the fit to the freespace regions compute in the calibration step and stored as an attribute of the `DiffractionLimitedProfile` class. We consider the ratio of $\hat{P}_0$ and the average noise to be SNR_0.

Following Equations 24-26 in Marouf et al. (1986) and Equations 26 and 27 in Asmar et al. (2018), we compute the threshold optical depth using

$$\tau_{TH} = -\sin(|B|)\ln\left[\frac{C_\alpha \dot{\rho}}{2\mathrm{SNR}_0 \Delta\rho}\right] \tag{8}$$

where B is the ring opening angle and $\dot{\rho}$ is the ring intercept radial velocity as computed by and attributed in the `Geometry` class, $C_\alpha = 2.41$ is chosen to correspond to 70% confidence[9], and $\Delta\rho$ is the radial spacing. For the DLP class, this is simply the `dr_km` positional argument specified when instantiating the DLP class and has a default of 0.25 km. For the reconstructed profile, $\Delta\rho$ will depend on the window size W and Fresnel scale F, the so-called *processing resolution* $\Delta R = 2F^2/W$.

4.5 Diffraction reconstruction routines

Symbol	Parameter Name	Attribute Name
ΔR	RECONSTRUCTION RESOLUTION (KM)	res
ρ	RING RADIUS	rho_km_vals
$\Delta\rho_{IP}$	RADIUS CORRECTION DUE TO IMPROVED POLE	rho_corr_pole_km_vals
$\Delta\rho_{TO}$	RADIUS CORRECTION DUE TO TIMING OFFSET	rho_corr_timing_km_vals
ϕ_{RL}	RING LONGITUDE	phi_rl_rad_vals
ϕ_{ORA}	OBSERVED RING AZIMUTH	phi_rad_vals
τ	NORMAL OPTICAL DEPTH	tau_vals
ϕ	PHASE SHIFT	phase_rad_vals
τ_{TH}	NORMAL OPTICAL DEPTH THRESHOLD	tau_threshold_vals
t_{OET}	OBSERVED EVENT TIME	t_oet_spm_vals
t_{RET}	RING EVENT TIME	t_ret_spm_vals
t_{SET}	SPACECRAFT EVENT TIME	t_set_spm_vals
B	OBSERVED RING ELEVATION	B_rad_vals
w	WINDOW WIDTH FOR RECONSTRUCTION	w_km_vals
f_{sky}	SKY FREQUENCY	f_sky_hz_vals
F	FRESNEL SCALE	F_km_vals
D	SPACECRAFT-RIP DISTANCE	D_km_vals
$\hat{T}$	DIFFRACTED COMPLEX TRANSMITTANCE	T_hat_vals
T	RECONSTRUCTED COMPLEX TRANSMITTANCE	T_vals

Table 8: Glossary of parameters contained in RSS_2005_123_X43_E_TAU_01KM.TAB. See companion label (.LBL) files for description of the data.

All of the diffraction reconstruction tools are located within the `diffrec` subpackage of `rss_ringoccs`. One can find simple tools for diffraction reconstruction of the diffraction pattern contained in an instance of the `NormDiff` class, as well as more complex tools for modeling problems and comparing them with real-world data and geometry. The main

[9]From Marouf et al. (1986) Equaiton 25, this is given by the root-mean-square of the difference between the measured complex signal $X = T + n$ (where n is the additive noise from the receiver) and actual complex signal T, normalized with respect to the expected receiver noise P_N.

dependency is the numpy package, but some functions also rely on tools found in the scipy package. The subpackage is broken into four submodules:

- `advanced_tools`
- `diffraction_correction`
- `special_functions`
- `window_functions`

The `diffraction_correction` submodule is the primary tool within `diffrec` and contains the `DiffractionCorrection` class, which is the main utility for creating diffraction-reconstructed profiles of radio occultation observations. The Python syntax is as follows:

```
In [1]: from rss_ringoccs import diffrec
In [2]: rec = diffrec.DiffractionCorrection(norm_inst, res)
```

Here, `norm_inst` is an instance of the `DiffractionLimitedProfile` class containing the diffracted data and `res` is the user-requested processing resolution of the reconstructed profiles in kilometers and expressed as a floating point number. There are several keywords in this class to allow the user to specify how the diffraction reconstruction will be performed.

A new feature of `rss_ringoccs` is the use of special polynomials within the diffraction reconstruction steps to greatly reduce computation time without sacrificing accuracy. The *Fresnel kernel*, $\psi(\rho, \rho_0; \phi, \phi_0)$, needs to be computed at its *stationary* value, ψ_s:

$$\frac{\partial \psi_s}{\partial \phi} = 0 \tag{9}$$

We expand ψ in a Taylor expansion about the point ϕ_0, and obtain the following:

$$\psi = \sum_{n=0}^{\infty} \psi^{(n)}(\rho, \rho_0; \phi_0, \phi_0) \frac{(\phi - \phi_0)^n}{n!} \tag{10}$$

The notation $\psi^{(n)}$ represents the n^{th} partial derivative of ψ with respect to ϕ. The tuple $(\rho, \rho_0; \phi_0, \phi_0)$ is to indicate that the coefficients of the Taylor expansion are *functions of the other variables*, and are not constants. We apply Newton-Raphson to find the stationary value of ψ, and obtain in the first perturbation the following value:

$$\phi_s = \phi_0 - \frac{\psi'(\rho, \rho_0; \phi_0, \phi_0)}{\psi''(\rho, \rho_0; \phi_0, \phi_0)} \tag{11}$$

Where, again, derivatives are taken with respect to ϕ. Truncating Eqn. 10 at the quadratic term, and evaluating at $\phi = \phi_s$, We obtain:

$$\psi_s \approx \psi(\rho, \rho_0; \phi_0, \phi_0) - \frac{1}{2} \frac{\psi'(\rho, \rho_0; \phi_0, \phi_0)^2}{\psi''(\rho, \rho_0; \phi_0, \phi_0)} \tag{12}$$

The nature of ψ allows for the right-hand side of Eqn. 12 to be expressed exactly in terms of Legendre polynomials. Stopping the Legendre expansion at the quadratic gives the classic *Fresnel Approximation*. This is:

$$\psi_s = \frac{\pi}{2} \left(\frac{\rho - \rho_0}{F} \right)^2 \tag{13}$$

For historical reasons and due to the use of Legendre polynomials, this is expansion is henceforth labelled as Fresnel-Legendre polynomials. `rss_ringoccs` allows for several different polynomial powers of this expansion by using the `psitype` keyword. This is a `string`, and the following inputs are allowed:

- 'Fresnel' - Classic Fresnel approximation.
- 'Fresnel3' - Legendre expansion up to the cubic term.
- 'Fresnel4' - Legendre expansion up to the quartic term.
- 'Fresnel6' - Legendre expansion up to the sextic term.
- 'Fresnel8' - Legendre expansion up to the octic term.
- 'Full' - No approximation, Newton-Raphson is applied.

For all but Rev133, the 'Fresnel4' option is more than adequate, and can reproduce the PDS results, as well as mimic the results obtained by using 'full'. As such, it has become the default in V1.1. For Rev133, a known problem with the cubic term of ψ persists, and the Fresnel-Legendre polynomials cannot adequately capture this. This is, in part, because the Fresnel-Legendre expansion assumes that the first iterate of the Newton-Raphson approximation is sufficient, whereas in such extreme geometries it is not. Below is a detailed description of the example included in the `quick_look_run.py` script discussed in Section 3.4. As with the quick-look script itself, this example assumes that the user has available the requisite `*.TAB` files generated by the example end-to-end script covered in Section 3.3. The `ExtractCSVData` class covered in the next section can be used to extract information from the `*.TAB` files and reconstruct the DLP instance `norm_inst`.

```
In [1]: geo = "../Data/GEO.TAB"
In [2]: cal = "../Data/CAL.TAB"
In [3]: dlp = "../Data/DLP.TAB"
In [4]: from rss_ringoccs.tools import ExtractCSVData
In [5]: from rss_ringoccs import diffrec
In [6]: norm_inst = ExtractCSVData(geo, cal, dlp, verbose=False)
In [7]: tau_inst_f = diffrec.DiffractionCorrection(
   ...: norm_inst, 1.0, rng="all", psitype="fresnel")
Computation Time: 12.491324
```

Note the quite short (12 second) reconstruction time, due in part to the 'Fresnel' setting for psitype and 1 km resolution. Running `DiffractionCorrection` with psitype='full':

```
In [8]: tau_inst_v = diffrec.DiffractionCorrection(
    data, 1.0, psitype="full", verbose=True)
    Things print out here...
Computation Time: 108.427886
In [9]: tau_inst = diffrec.DiffractionCorrection(
    data, 1.0, psitype="full")
Computation Time: 76.470007
```

There are several things to note here. The computation of ψ is one of the slowest parts in the entire diffraction reconstruction algorithm. In particular, the computation of the

stationary phase can be quite time-consuming. Since 'Fresnel' skips all of this, we see a substantial reduction in computation time. The data set that was used in this example comes from the Cassini rev007E occultation observation. We can check the validity of Fresnel approximation for this set by looking at the difference in the two reconstructions. Note that since the power is normalized to 1, this is both fractional and absolute error:

```
In [10]: import numpy as np
In [11]: np.max(np.abs(recf.power_vals-rec.power_vals))
Out[11]: 0.00016784579326811766
In [12]: np.mean(np.abs(recf.power_vals-rec.power_vals))
Out[12]: 3.5374768401331293e-06
```

The Fresnel approximation works very well here. The default setting of psitype='Fresnel4' is slightly slower than 'Fresnel', but still finishes execution in less than 20 seconds. For many occultations where 'Fresnel' fails, 'Fresnel4' still produces accurate results. Another thing to note is that there is a large discrepancy in the computation time for when verbose=True and verbose=False is set. Since verbose prints out pieces of information for every point that is being reconstructed, the Python interpreter needs to wait for the line to be printed before it can process the next point. In most cases this is not an issue, but when speed is crucial it may be better to leave verbose set to False.

4.6 Utility routines

Within the `tools/` subpackage one can find various `pds3_*_series.py` scripts and routines to read and write PDS3-type data and label files.[10] `rss_ringoccs` manages the file naming conventions and calling of the `pds3_*_series.py` scripts by means of the `write_output_files.py` script.

Also included as a utility for the quick-look pipeline is the `ExtractCSVData`, a tool for extracting information from the `*.TAB` files and reconstructing the DLP instance `norm_inst`. This can be found in the `CSV_tools` submodule of the `tools` subpackage, all contained within `rss_ringoccs`. The steps for importing are shown below.

The `ExtractCSVData` imports user-specified `*.TAB` files produced by the end-to-end pipeline and uses them to construct an instance of the `NormDiff` class that can then be passed on for diffraction reconstruction as a part of the quick-look process. This way, the pipeline only needs to be run once on a given data set, and then the user may experiment with different resolutions, window functions, etc., on the diffracted data without repeated time consuming steps. For example, from the master directory of `rss_ringoccs`, one could use ipython to implement the following to construct a `DiffractionLimitedProfile` instance from `*.TAB` files output from a previous run:

[10]The products of these routines have not been thoroughly checked for PDS3 compliance.

```
cd ~/Research/rss_ringoccs-master
ipython
In [1]: path ='../output/Rev007/E/Rev007E_RSS_2005_123_X43_E/'
In [2]: geo = path+'RSS_2005_123_X43_E_GEO_20180926_0001.TAB'
In [3]: cal = path+'RSS_2005_123_X43_E_CAL_20180926_0001.TAB'
In [4]: dlp = path+'RSS_2005_123_X43_E_DLP_0100M_20180926_0001.TAB'
In [5]: from rss_ringoccs.tools.CSV_tools import ExtractCSVData
In [6]: from rss_ringoccs import diffrec
In [7]: dlp_inst = ExtractCSVData(geo, cal, dlp, verbose=True)
Extracting Data from CSV Files:
    Extracting Geo Data...
    Geo Data Complete.
    Extracting Cal Data...
    Cal Data Complete.
    Extracting DLP Data...
    DLP Data Complete
    Retrieving Variables...
    Computing Variables...
    Interpolating Data...
    Data Extraction Complete.
    Writing History...
    History Complete.
    Extract CSV Data Complete.
```

Also note that it is possible to combine `*.TAB` files from different end-to-end runs of `rss_ringoccs`, which is encouraged for users who want to examine the effect different calibration inputs might have on the final reconstructed optical depth profile.

The `CompareTau` tool, found in the `advanced_tools` submodule of the `diffrec` subpackage, imports user-specified `*.TAB` files produced by the end-to-end pipeline and runs the diffraction reconstruction at an additional user-specified spatial resolution for the purpose of comparing optical depth profiles for the same occultation with the only difference being the processing resolution.

4.6.1 PDS3Reader

The `PDS3Reader` function allows users to easily read in a set of PDS3-formatted data and label files without having to scroll through and examine a label file in detail (for column headers, etc.). To use the function, first verify that the desired data and label file are within the same directory. Then, follow the example below but replace `lbl_file` with the path to the desired label file.

```
ln [1]: import rss_ringoccs as rss
ln [2]: lbl_file = 'RSS_2005_123_X43_E_GEO_20180926_0001.LBL'
ln [3]: geo = rss.tools.PDS3Reader(lbl_file, use_attr_names=False)
```

The `geo` variable will contain two classes as attributes: `series` and `keywords`. `series` refers to the actual data set, and calling `geo.series.__dict__.keys()` will print all the data column headers, as seen in the label file. By setting the keyword argument `use_attr_names` to `True`, these column header names will be replaced by the attribute name used in `rss_ringoccs` to represent the same variable (see Tables 5-7). To grab the data associated with the column header, simply call `geo.series.XX`, where `XX` is the header name. `keywords` contains all of the keywords listed in the label file, and the corresponding keyword values can be called in a similar fashion: `geo.keywords.XX`,

where XX is the keyword name. Definitions to these keywords should be available on the PDS data dictionary https://pds.nasa.gov/tools/dd-search/.

4.6.2 Label History

Each label file produced by rss_ringoccs will contain a PROCESSING_HISTORY_TEXT that lists user information (such as Python version, operating system, etc.) as well as an accumulated list of all positional and keyword arguments that were used to run the pipeline up to part where the label was created. Users can visually read this list and rerun the pipeline to reconstruct the same profile. Alternatively, users can use the read_history function, which will automatically read in the listed inputs and output a requested instance, if available. For example, a *TAU.LBL file will contain all of the inputs to the RSRReader, Geometry, Calibration, DiffractionLimitedProfile, and DiffractionCorrection classes. Using read_history on the *TAU.LBL will give users the option of returning an instance of any of the above classes.

This function is useful in particular for those who wish to reproduce a dlp_inst sampled at finer radial intervals.

5 Validation of rss_ringoccs algorithms

Here we present tests and validations of the performance and output of rss_ringoccs. Perhaps most significantly, this includes a comparison of rss_ringoccs results with those published on the PDS as these results were processed using state-of-the-art methods following Marouf et al. (1986). This includes a demonstration of the results for Cassini and for Voyager, as well as reproduction of analytical solutions, results from raw data sampled at different rates, and results from DLPs sampled at different rates.

5.1 Comparison with results on PDS

5.1.1 Cassini RSS results

The results of rss_ringoccs match those in PDS CORSS_8001 extremely well. After completing the Huygens ringlet end-to-end example in Section 3.3, several data products will be created. In Figs. 6-7, we compare our output GEO file, plotted in blue, with the PDS GEO file, plotted in dashed red lines. These values are, for our purposes, essentially the same – the comparisons without grey dots indicating a fractional error match exactly to the precision listed in the files.

The calibration steps require more complex calculations and some user judgment and thus our results do not match the PDS as well as the geometry does, but overall these differences are small and almost unavoidable. A major part in the calibration step is to normalize the signal power such that it reaches unity within free-space regions, but the fit type and order rely heavily on user choices (see sec xx). So, even though Figure 9 looks as though the signal power outside of the ring system is at unity, indicating a good fit, if we zoom into a feature and compare our final signal power to that on the PDS, the unity background signals are slightly offset. This is seen in the Maxwell ringlet but not the Huygens ringlet.

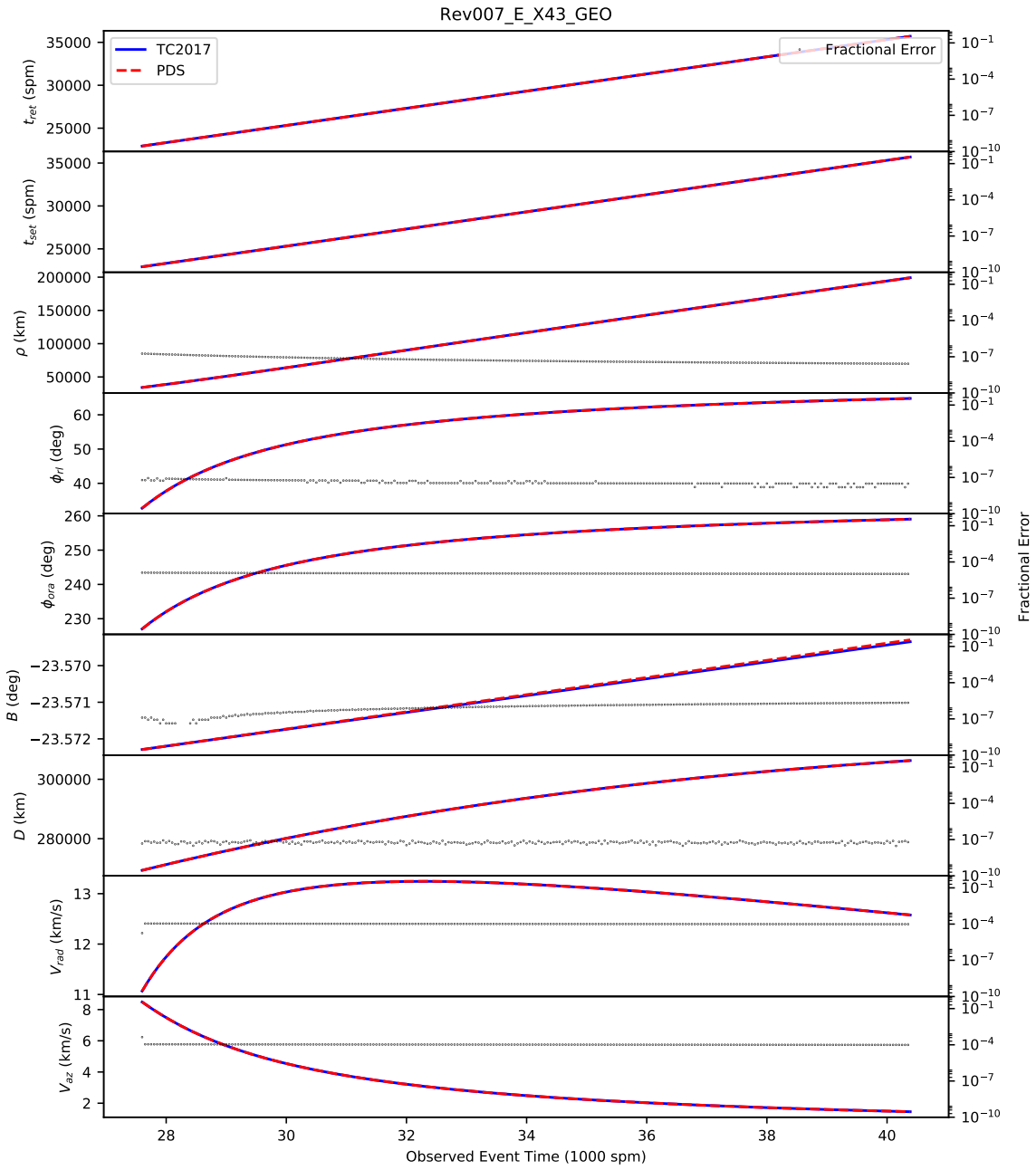

Fig. 6: Comparison of geometry parameters for Rev007 Egress X-band as viewed from DSS-43. PDS `CORSS_8001` data product `Rev007/Rev007E/Rev007E_RSS_2005_123_X43_E/RSS_2005_123_X43_E_GEO.TAB` values are plotted in dashed red lines, with `rss_ringoccs` values overplotted in blue. Fractional error between the two are plotted on the right-hand y-axis in grey dots.

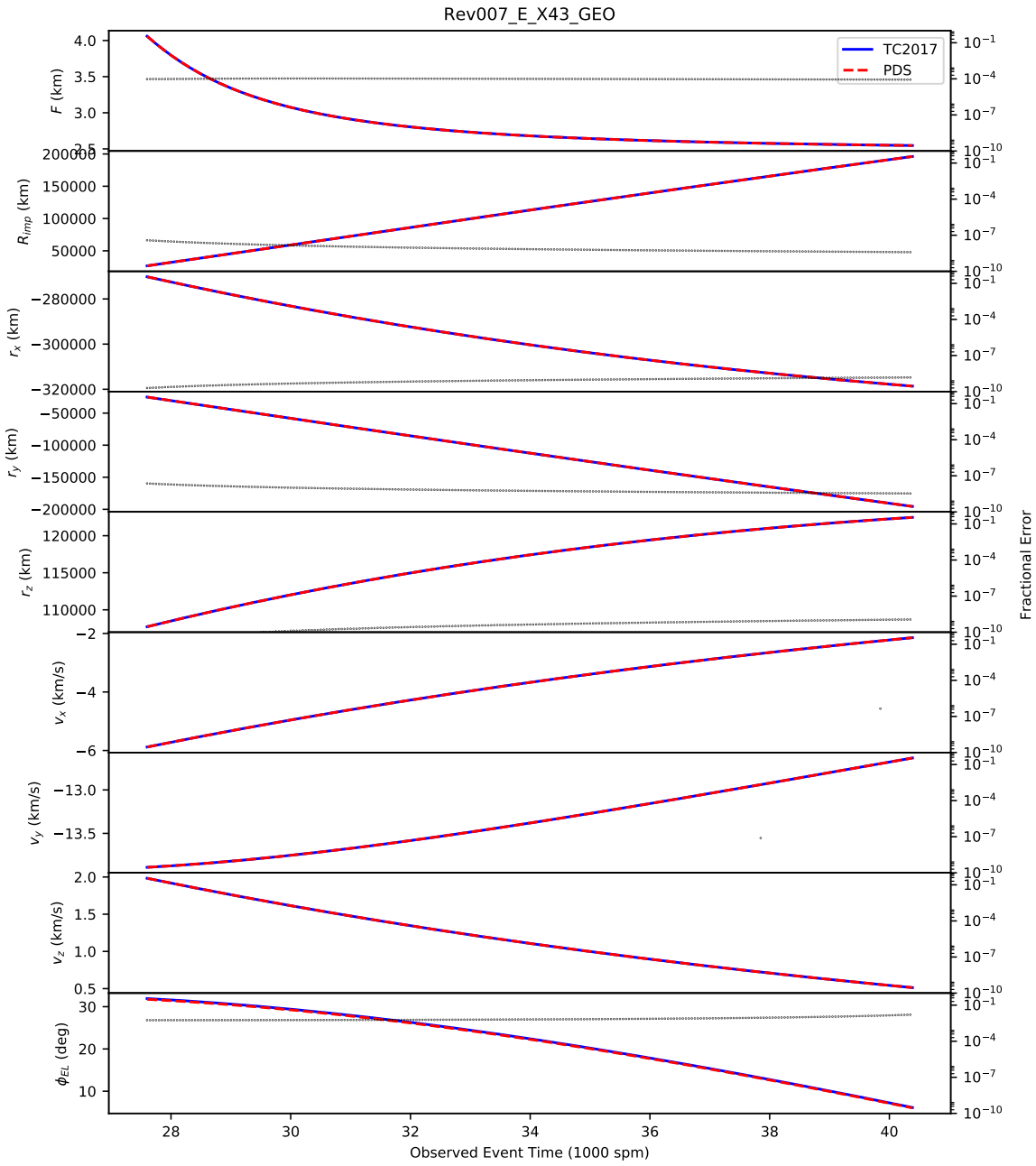

Fig. 7: Comparison of geometry parameters for Rev007 Egress X-band as viewed from DSS-43. PDS `CORSS_8001` data product `Rev007/Rev007E/Rev007E_RSS_2005_123_X43_E/RSS_2005_123_X43_E_GEO.TAB` values are plotted in dashed red lines, with `rss_ringoccs` values overplotted in blue. Fractional error between the two are plotted on the right-hand y-axis in grey dots.

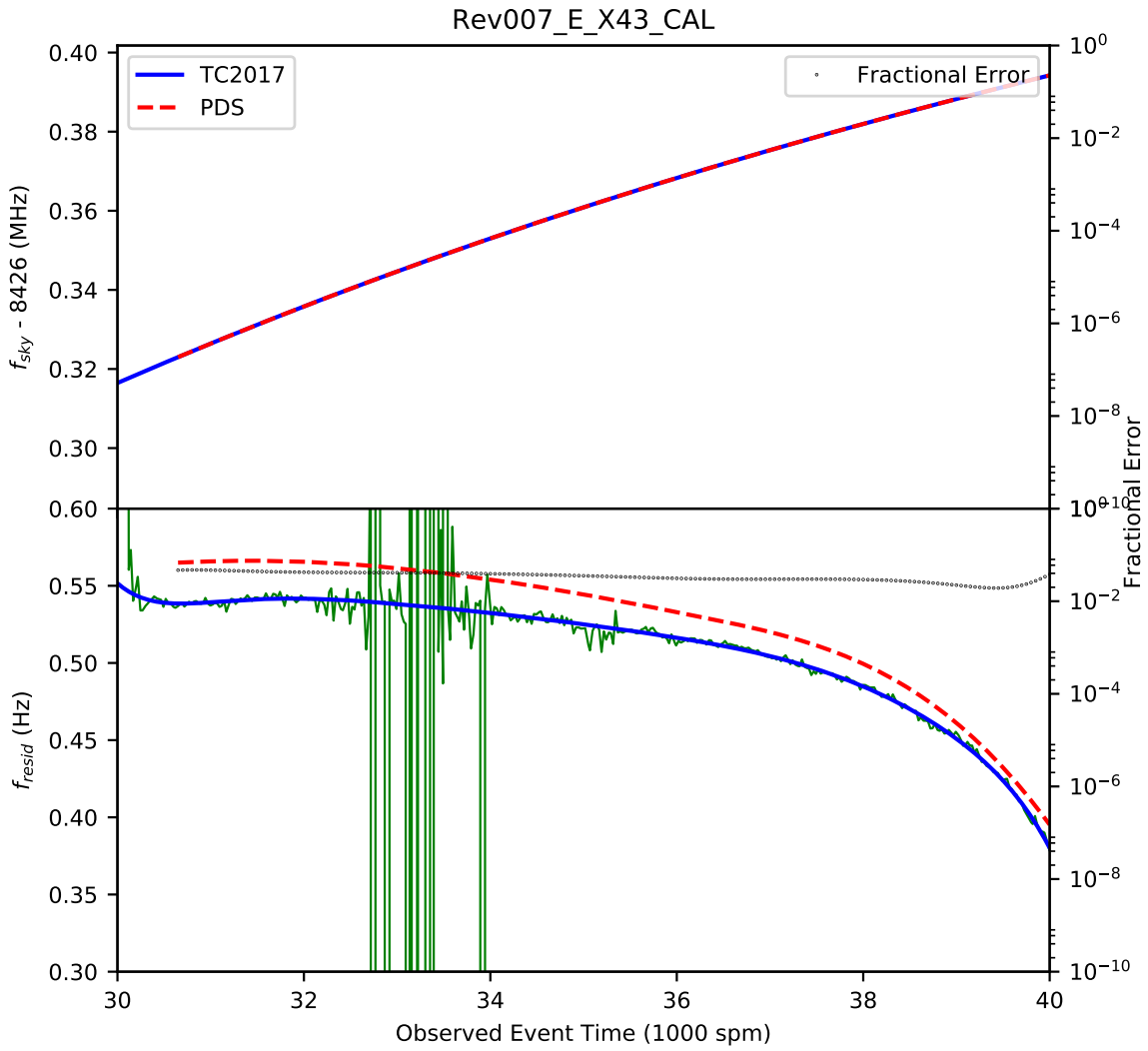

Fig. 8: Comparison of the Frequency Offset and Residual Frequency computed for the Rev007 E X43 data set.

If Fig. 8 we plot the output of the calibration steps of the pipeline for the Rev007 E X43 data set. Plotted with this are the results found on the PDS, as well as the fractional error between the two. Below in Fig. 9 we plot the raw power that is extracted from the RSR files:

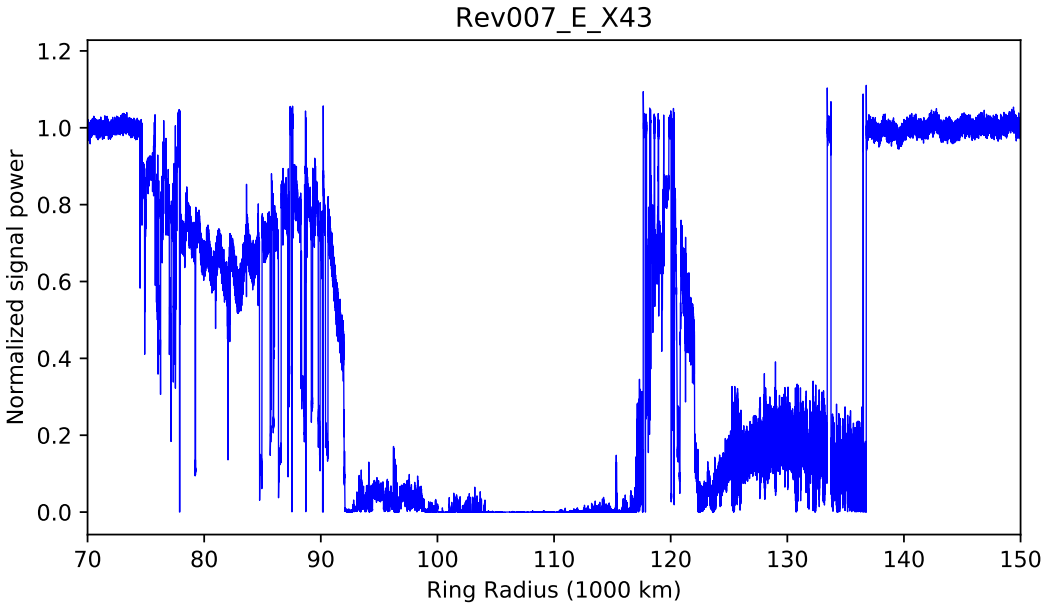

Fig. 9: Raw Power from Rev007 E X43

Finally, at the end of the pipeline we obtain the reconstructed profiles of the Saturnian ring system. It is important to note that the normalization step can be very subtle. As an example of this, we show the reconstruction of Rev007 E X43 in Fig 10 about the Huygens ringlet and the Maxwell ringlet. The default fit was used to create the normalized power. The fit and reconstruction worked extremely well for Huygens, but there is a slight discrepancy for the Maxwell ringlet. Adjusting the polynomials used in the spline fit will alleviate this error, and it is up to the user to decide when the fit is sufficient for their needs.

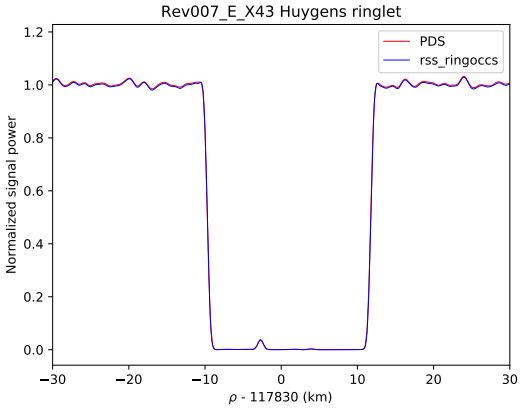

10.1: Huygens ringlet reconstructed normalized power.

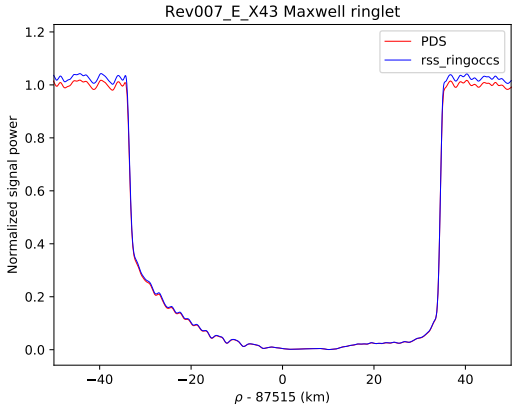

10.2: Maxwell ringlet reconstructed normalized power.

Fig. 10: Comparison of reconstructed normalized power with PDS results. PDS results are plotted in red and can be found from `Rev007/Rev007E/Rev007E_RSS_2005_123_X43_E/RSS_2005_123_X43_E_TAU_01KM.TAB`). `rss_ringoccs` results are in blue.

5.2 Effect of different sampling rates

The raw data recorded at the DSN stations are sampled at 16 kHz. The high resolution of these data poses two difficulties: (i) each RSR data file is at least many hundreds of

megabytes in size for an ingress or egress diametric occultation (chord occultations are even larger), which can be cumbersome especially for users downloading a large number of RSR files; (ii) the `rss_ringoccs` processing time on a conventional laptop for each data file can be at least thirty minutes for diametric occultation (even longer for chord occultations), which is particularly computationally expensive for users looking to reduce data for numerous occultations. The PDS provides RSR data files with the raw data down-sampled to 1 kHz. These files are twelve to sixteen times smaller (lower limit of tens of megabytes instead of hundreds) and take 90 to 180 seconds for `rss_ringoccs` to process.

The computational benefits of utilizing the 1 kHz files over the 16 kHz files is clear. However, we must demonstrate that the down-sampled data yield results comparable to those of the raw high-resolution data. To begin this validation, we process 1 kHz and 16 kHz data files for X band at high ring opening angle ($B \approx 23°$) and Ka band at low ring opening angle ($B \approx 5°$). Then, we compare and contrast the 1 kHz and 16 kHz processing results from the calibration, DLP, and reconstruction steps as shown in Fig. 11.

The frequency offset residuals and freespace power fits differ by less than 0.1% within the ring system, while the computed frequency offsets differ by less than 0.01%. The DLP optical depth values are typically within 0.01 dB of one another, although this is not the case for the part of the profile associated with the B ring. Any differences seen between the two profiles can be ascribed to changes in the diffraction pattern when the profile is down-sampled to the DLP radial sampling resolution. This assertion is substantiated by the similarity of the diffraction-corrected optical depth profiles. Because the diffraction reconstruction eliminates diffraction patterns in the profile, the excellent agreement of the two reconstructed profiles indicates that the disparity between the DLP optical depths is due to differences in the diffraction patterns.

Having been demonstrated to yield results comparable to those from the 16 kHz files, the 1 kHz files are recommended for processing instead of the 16 kHz files. Users can obtain 1 kHz files for the majority of occultations from the PDS with only a few exceptions. In these cases, we recommend the user decimate the 16 kHz file to 1 kHz at the start of the pipeline by setting the `decimate_16khz_to_1khz` keyword argument equal to `True`.

6 Where to go from here

6.1 The Cassini RSS data catalog

We have created a `CSV` file, located within the `tables` directory, with all 1 kHz Cassini ring occultation RSR files available on the PDS. This catalog includes information of each RSR file, such as wavelength/frequency band, observing station information, sampling rate, associated kernels, etc., as well as relevant geometry parameters that can help users determine which file they want to use. The column headers and definitions for this catalog are also available within the `tables/` directory.

6.2 Selecting an RSR file to process

Before using `rss_ringoccs`, we recommend users browse the Cassini RSS data catalog to find an appropriate RSR file to process. Factors such as elevation angle, antenna size, radius range, and ring opening angle can affect this decision.

First, users should establish that the RSR file covers the radius range of interest. Some occultations, such as chords, do not cover the entire ring system (see Figure 22.2). Next, depending on the research goal, users should select an observation with the desired ring opening angle. A large ring opening angle means that the spacecraft signal has gone through less ring material, and a small ring opening angle means that the signal has gone through more ring material. The latter is useful for tenuous features, such as some C ring density waves, and the former is useful for observing optically thick regions, such as the B ring. Another factor to consider is the Earth receiving station. Different stations will record in different bands (S-, X-, or Ka-band) using different sized antennas (34m or 70m). The location of the DSN is also important, as Cassini could be lower in the sky at one station but higher in the sky at another – this affects the amount of atmosphere the signal must go through to reach the station. These station-related factors can affect the overall SNR as well as the background power drift.

6.3 Choosing a radial resolution

As discussed in Secion 3.6, users must provide the shortest resolvable wavelengths to `rss_ringoccs` in the form of radial sample spacing in km for both the DLP and the reconstructed profile. The latter must always be at least 8/3 greater than the former; however, there are additional considerations in choosing a sample spacing.

In Figure 8, Marouf et al. (1986) show a relation between threshold optical depth τ_{TH} (Section 4.4.1) and processing resolution ΔR for X and S band. Because lower resolutions lead to larger SNR values, τ_{TH} increases with ΔR. If the intrinsic SNR is low–more often the case in Ka band or low-elevation observations with large Earth atmosphere extinction– a small radial sampling rate might not produce meaningful results because the profile normal optical depth frequently exceeds the threshold optical depth. In such cases, we recommend users consider the threshold optical depth when selecting the shortest resolvable wavelength.

6.4 Execution time benchmarks

The single-file end-to-end example script discussed in §3.3 includes a benchmark computation time for a typical 1 kHz RSR file for a diametric occultation. When run, `e2e_run.py` will print out the expected processing time for a single 1 kHz RSR file. We have conducted a series of benchmarks for various machines across a range of hardware and operating systems and various resolvable wavelengths. The results of these benchmark runs for a single 1 kHz file are listed below for reference. Note that processing time may vary based on other tasks being run by a machine at the time of running `rss_ringoccs`. For our own benchmarks, we find benchmark times can vary by up to ≈5% for a given machine.

4/3ΔR (km)	$\Delta\rho$ (km)	Time (s)
MacBook Pro, 2.9 GHz Intel Core i7, 16GB RAM		
0.25	1.0	90
0.25	0.667	120
0.05	0.25	270
0.05	0.134	400

Table 9: Benchmarks for processing the Rev 007 E X43 1 kHz RSR file.

In addition to these individual benchmarks, we have run a benchmark of the batch processing script. A complete run of `e2e_batch.py` which processes all 1 kHz RSR files before USO failure requires 5.25 hrs to run on with a 2.9 GHz Intel Core i7 CPU with 16 GB of RAM and ≈10 hrs with a 2.7 GHz Intel Core i5 CPU and 8 GB RAM.

6.5 Licensing

`rss_ringoccs` is free/open-source software made available under the GNU General Public License. The following license is included with the top-level `__init__.py` file in the `rss_ringoccs` software package:

```
Copyright (C) 2018 Team Cassini at Wellesley College

This program is free software: you can redistribute it
and/or modify it under the terms of the GNU General Public
License as published by the Free Software Foundation,
either version 3 of the License, or (at your option) any
later version.

This program is distributed in the hope that it will be
useful, but WITHOUT ANY WARRANTY; without even the implied
warranty of MERCHANTABILITY or FITNESS FOR A PARTICULAR
PURPOSE. See the GNU General Public License for more
details.

You should have received a copy of the GNU General Public
License along with this program. If not, see
http://www.gnu.org/licenses/.

This program is part of the rss_ringoccs repository hosted
at https://github.com/NASA-Planetary-Science/rss_ringoccs
and developed with the financial support of NASA's Cassini
Mission to Saturn.
```

6.6 Citing `rss_ringoccs`

If you use `rss_ringoccs` in your research as the basis of a publication, please consider citing the software package using the DOI:10.5281/zenodo.2548947

Acknowledgements

Development of `rss_ringoccs` was supported by NASA/JPL as part of the Cassini Mission Closeout effort. The authors especially appreciate the support and encouragement of Linda Spilker and Kathryn Weld. We dedicate this work to the memory of Arv Kliore, the original Cassini RSS Team Leader and an example of wisdom and generosity for us all.

Appendices

A Meta-kernel file

A meta-kernel file contains a list of the complete pathnames to a list of individual kernel files. An example meta-kernel `Rev007_meta_kernel` has been provided in the `./examples/` directory for the Rev007 occultations. To create a meta-kernel for another occultation, follow the structure of the Rev007 meta-kernel example. Typically, the only files one needs to change are those with a `*.bsp` or `*.tpc` extension. All kernel files necessary for building the meta-kernel for a specific observation are listed in final column of the data catalog found in the `./tables/` directory. For example, the Rev014 occultation might have a meta-kernel with the following contents:

```
\begindata
PATH_VALUES  = ( '../kernels/naif/CASSINI/kernels/spk'
                 '../kernels/naif/CASSINI/kernels/lsk'
                 '../kernels/naif/generic_kernels/spk/planets'
                 '../kernels/naif/generic_kernels/spk/stations'
                 '../kernels/naif/generic_kernels/pck'
                 '../kernels/naif/CASSINI/kernels/pck'
                 '../kernels/local')

PATH_SYMBOLS = ('A', 'B', 'C', 'D', 'E', 'F', 'G')

KERNELS_TO_LOAD = ( '$A/051011R_SCPSE_05245_05257.bsp'
                    '$B/naif0012.tls'
                    '$C/de430.bsp'
                    'F/cpck11Oct2005.tpc'
                    '$D/earthstns_itrf93_050714.bsp'
                    '$F/earth_000101_180919_180629.bpc')

\begintext
These are the kernels used for Rev014
```

B Calibration Output Plots

After computing $\hat{f}(t)_{resid}$ from the frequency offset residual, the `FreqOffsetFit` class plots $f(t)_{resid}$, the $f(t)_{resid}$ values used to compute $\hat{f}(t)_{resid}$, and $\hat{f}(t)_{resid}$, along with labels specifying the polynomial order used in the fit, information identifying the revolution number, direction, wavelength band, DSN station, processing date, and processing serial number. `FreqOffsetFit` saves this plot in a PDF in the directory within `./output/` corresponding to the current Rev, band, and DSN station. This is the same directory as the `.LBL` and `.TAB` files output by `rss_ringoccs` if `write_file` is set to `True` (the recommended value). The output PDF is named following the same conventions as the `.LBL` and `.TAB` files, complete with processing date and serial number. We show an example of one such output plot in Figure 12 for the occultation Rev 007 in the egress direction as observed in the X-band from DSN station 43.

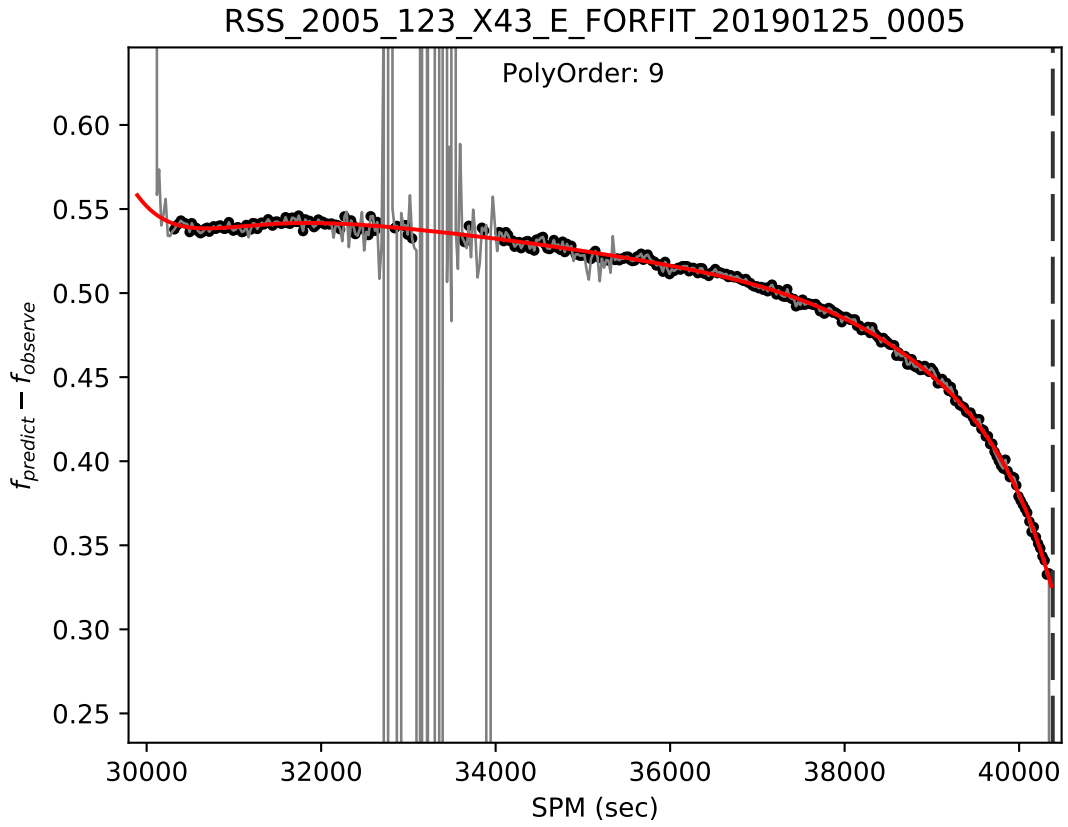

Fig. 12: Example of the frequency offset residual fit plot output by the `FreqOffsetFit` submodule of `Calibration` step. The total frequency offset residual $f(t)_{resid}$ is depicted in grey, the $f(t)_{resid}$ used to compute $\hat{f}(t)_{resid}$ in black, and the fit $\hat{f}(t)_{resid}$ in red.

After computing $\hat{P}_0$ from available freespace regions, the `Normalization` class plots power, the power values used to compute $\hat{P}_0$, and $\hat{P}_0$, along with labels specifying the fit type, fit order, and information identifying the revolution number, direction, wavelength band, DSN station, processing date, and processing serial number. `Normalization` saves this plot in a PDF in the directory within `./output/` corresponding to the current Rev, band, and DSN station. This is the same directory as the `.LBL` and `.TAB` files output by `rss_ringoccs` if `write_file` is set to `True` (the recommended value). The output PDF is named following the same conventions as the `.LBL` and `.TAB` files, complete with processing date and serial number. We show an example of one such output plot in Figure 13 for the occultation Rev 007 in the egress direction as observed in the X-band from DSN station 43.

C Interactive Mode

When the `interact` keyword argument is set to `True` when instantiating the `Calibration` object class, the free space power fitting method will enter interactive mode to receive user input. After the initial automated fit to the free space regions, `rss_ringoccs` will plot the results of the fit (in the same manner as Figure 13) in a `matplotlib` window and prompt the user for input in the terminal.

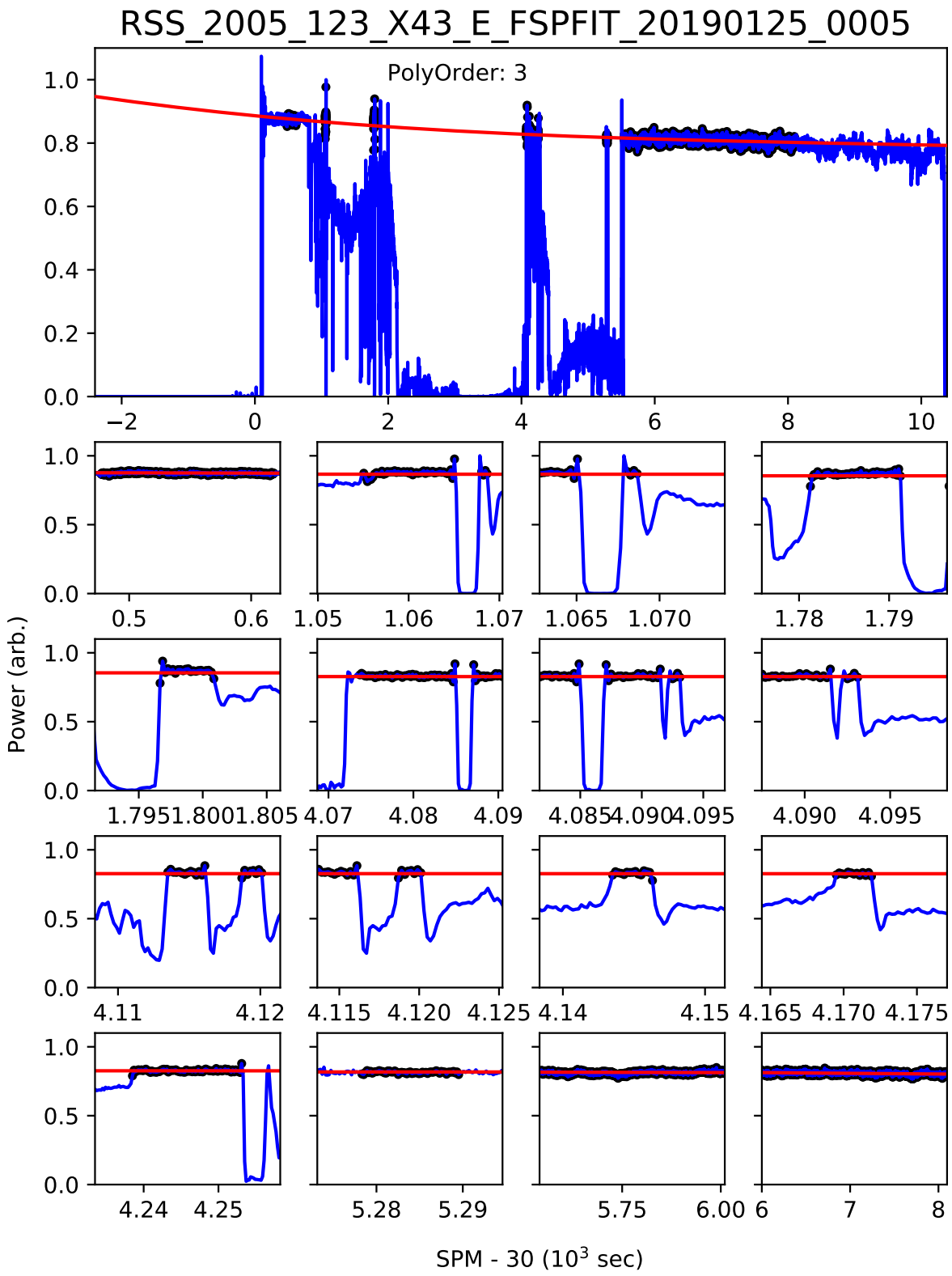

Fig. 13: Example of the free space power fit plot output by the `Normalization` submodule of `Calibration` step. Phase-detrended power is shown in blue, the power used to compute the fit $\hat{P}_0$ to the free space power in black, and the fit $\hat{P}_0$ in red. Top panel is the total power profile. Each subpanel is a closeup of one of the free space regions used in the fit. Subpanels shown in order of time observed (SPM). The number of subpanels will vary depending on the number of freespace regions used in the fit.

Here, we explain the input at each prompt and then show an example of a single iteration of the interactive mode with possible responses.

```
Do you want to continue with this fit? (y/n): n

Do you want to change the freespace regions? y


Last used freespace gaps in SPM:
[[30477.0, 30618.833698196322],
[31054.928062871928, 31065.345792559005],
[31067.770358800513, 31068.930045219375],
[31780.866566933848, 31791.436274129595],
[31796.580066071256, 31801.05616095102],
[34073.68113956013, 34085.4943434775],
[34086.68935725464, 34091.74708080809],
[34092.49215200969, 34093.327481330285],
[34113.3838723948, 34116.39786534125],
[34118.619852169526, 34120.21853934005],
[34143.358694145434, 34146.38873649045],
[34169.41951728726, 34172.05701601253],
[34238.49233676398, 34253.26244631217],
[35278.146362236446, 35289.59914281318],
[35545.59294280804, 36005.16144320606],
[36005.16144320606, 38092.48430556758]]


Do you want to revert to the default freespace gaps?  n
Please input new freespace gaps in SPM and press enter twice:
[[30477, 30618],[31055, 31065],[34087, 34091],[34114, 34116],
[35546, 36005],[36006, 38092]]

[[30477, 30618],
[31055, 31065],
[34087, 34091],
[34114, 34116],
[35546, 36005],
[36006, 38092]]

What fit type would you like to use? (poly/spline): poly

What fit order would you like to use?: 3

Do you want to continue with this fit? (y/n): n
```

1. Entering `y` will end interactive mode and accept the current fit. Type `n` to continue interactive mode and change the fit properties.
2. `n` will skip the prompt for new free space regions. `y` will continue to the prompt for reverting to original free space regions.
3. `y` will revert the free space regions to those predicted by the `Geometry` class and skip the prompt for new free space regions. `n` will continue to a prompt for new, user-defined free space regions.
4. User now enters a 2xN list of floats specifying the desired free space regions in SPM (units of seconds). N must be greater than or equal to five in order for the free space fitting to properly select the data in the free space regions. For clarity and verification, the entered freespace regions will be printed to the terminal after the user input is parsed.

5. Enter the type of fit to use for the freespace power. Two fit types are available, a spline (`spline`) and a polynomial (`poly`); however, we highly recommend the polynomial fit.
6. Enter a whole number between 1 and 9 for polynomial fit or between 1 and 5 for spline fit.
7. A plot of the new fit made based on the user input will appear in a `matplotlib` window. The interactive mode will return to the initial prompt about whether to accept the fit or to continue with interactive mode. Return to step 1.

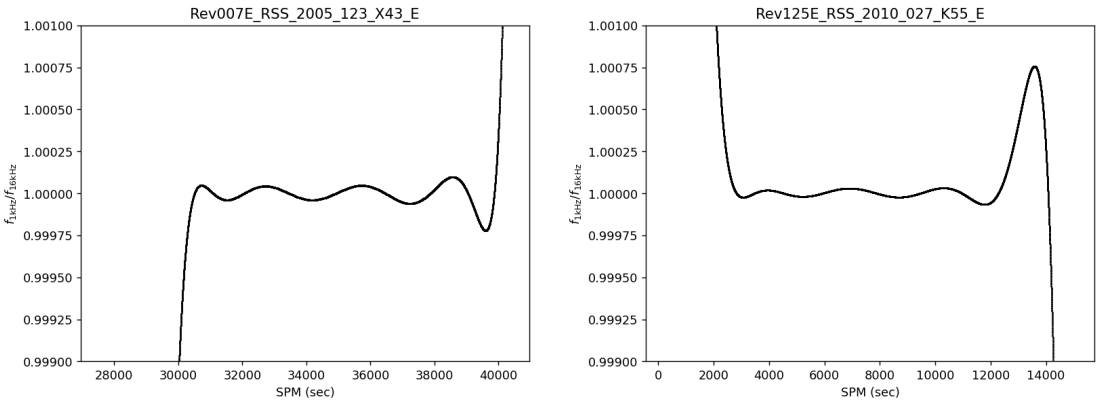

11.1: Ratio of 1 kHz to 16 kHz Frequency Offset Residual Fits.

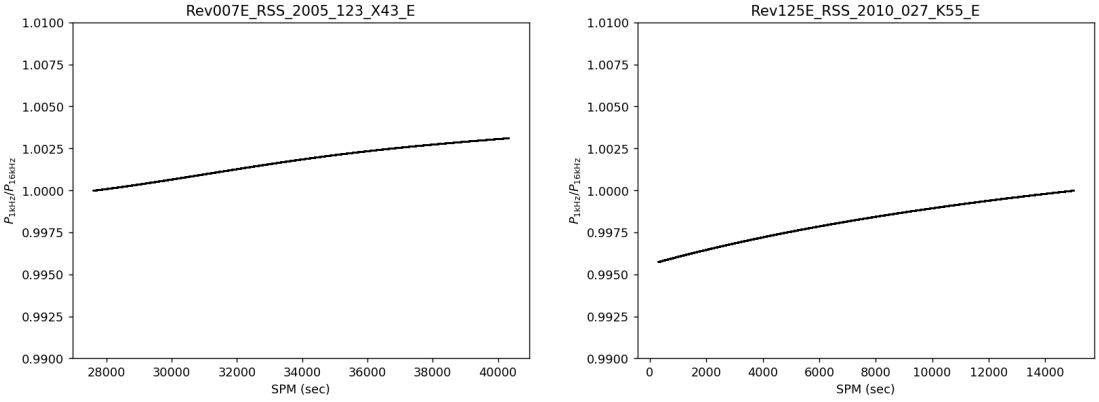

11.2: Ration of 1 kHz to 16 kHz Free Space Power Fits.

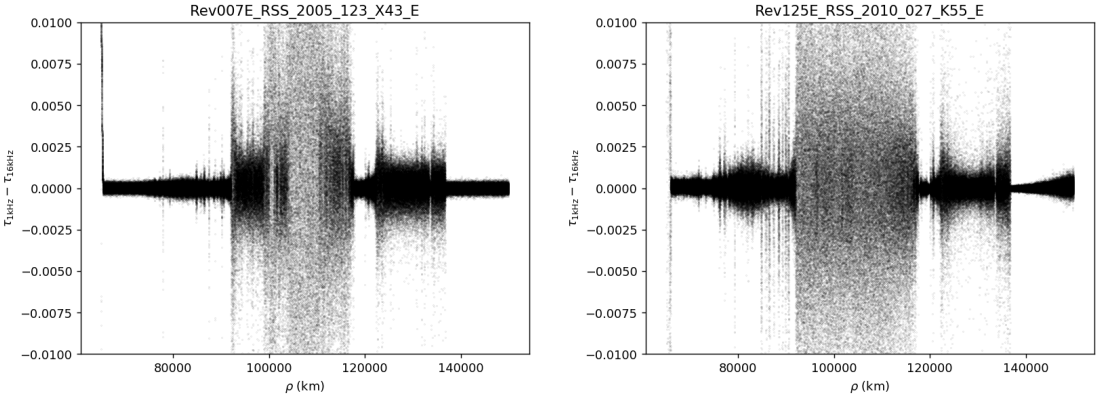

11.3: Difference between 1 kHz and 16 kHz DLP optical depths.

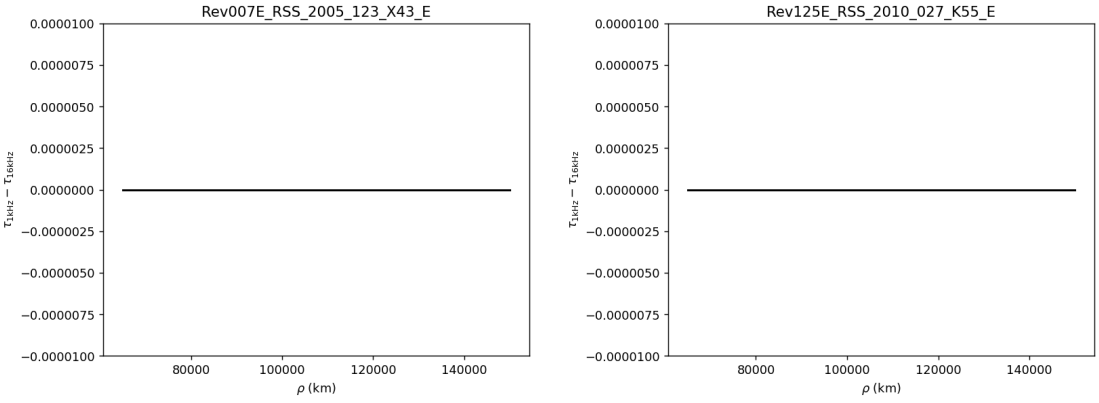

Fig. 11: Validation of 1 kHz processing using raw 16 kHz processing for Rev 007 E X band and Rev 125 E Ka band.

Acronyms

DSN Deep Space Network. 2

HGA High Gain Antenna. 2

NASA National Aeronautic and Space Administration. 1

PDS Planetary Data System. 1

RSR Radio Science Receiver. 3, 5

RSS Radio Science Subsystem. 1

Glossary

Atmospheric occultation
Disappearance or reappearance of a source after the signal has passed through the atmosphere of a planet or satellite. 2

Chord occultation
Ring occultation. 3

Deep Space Network
NASA's complex of Earth-based antennas, used to communicate with spacecraft. 2

Diametric occultation
An occultation geometry in which the path of the complete occultation extends from ring ansa to ring ansa, passing behind the planet at mid-occultation. 2

Diffraction Reconstruction
Retrieval of radial optical depth profile of Saturn's rings responsible for observed diffraction pattern. 2

Egress
Exit phase of a ring or atmosphere occultation. 2

Fresnel inversion
Retrieval of intrinsic optical depth profile of the rings by using a Fresnel transform to correct for the effects of diffraction in the observed signal. 2

High Gain Antenna
Highly directional main spacecraft antenna for communications and radio science. 2

Ingress
Entry phase of a ring or atmosphere occultation. 2

NASA
National Aeronautics and Space Administration. 1

Planetary Data System
Long-term archive of digital data products returned from NASA's planetary missions, and from other kinds of flight and ground-based data acquisitions. 1

Radio Science Receiver
An open-loop receiver used in NASA's Deep Space Network (DSN) facilities. 3, 5

Radio Science Subsystem
A subsystem placed on board a spacecraft for radio science purposes. 1

Rev number
The number of times the Cassini spacecraft has orbited Saturn. 2

References

Acton, C. (1996), 'Ancillary Data Services of NASA's Navigation and Ancillary Information Facility', *Planetary and Space Science* **44**, 65–70.

Asmar, S. W., French, R. G., Marouf, E. A., Schinder, P., Armstrong, J. W., Tortora, P., Iess, L., Anabtawi, A., Kliore, A. J., Parisi, M., Zannoni, M., & Kahan, D. (2018), *Cassini Radio Science User's Guide*, v1.1 edn, NASA Jet Propulsion Laboratory.

Colwell, J., Nicholson, P., Tiscareno, M., Murray, C., French, R. & Marouf, E. (2009), 'The Structure of Saturn's Rings', *Saturn from Cassini-Huygens* p. 375.

French, R., McGhee-French, C., Lonergan, K., Sepersky, T., Jacobson, R., Nicholson, P., Hedman, M., Marouf, E. & Colwell, J. (2017), 'Noncircular features in Saturn's rings IV: Absolute radius scale and Saturn's pole direction', *Icarus* **290**, 14–45.

French, R., Nicholson, P., Hedman, M., Hahn, J., McGhee-French, C., Colwell, J., Marouf, E. & Rappaport, N. (2016a), 'Deciphering the embedded wave in Saturn's Maxwell ringlet', *Icarus* **279**, 62–77.

French, R., Nicholson, P., McGhee-French, C., Lonergan, K., Sepersky, T., Hedman, M., Marouf, E. & Colwell, J. (2016b), 'Noncircular features in Saturn's rings III: The Cassini Division', *Icarus* **274**, 131–162.

Kliore, A., Anderson, J., Armstrong, J., Asmar, S., Hamilton, C., Rappaport, N., Wahlquist, H., Ambrosini, R., Flasar, F., French, R., Iess, L., Marouf, E. & Nagy, A. (2004), 'Cassini Radio Science', *Space Science Reviews* **115**, 1–70.

Marouf, E., French, R., Rappaport, N., Wong, K., McGhee-French, C. & Anabtawi, A. (2011), 'Uncovering of small-scale quasi-periodic structure in Saturn's ring C and possible origin', *EPSC-DPS Joint Meeting* **265**.

Marouf, E., Tyler, L. & Rosen, P. (1986), 'Profiling Saturn's rings by radio occultation', *Icarus* **68**, 120–166.

Moutamid, M. E., Nicholson, P., French, R., Tiscareno, M., Murray, C., Evans, M., French, C., Hedman, M. & Burns, J. (2016), 'How Janus' orbital swap affects the edge of Saturn's A ring?', *Icarus* **279**, 125–140.

Nicholson, P., French, R. & Colwell, M. H. E. M. J. (2014a), 'Noncircular features in Saturn's rings I: The edge of the B ring', *Icarus* **227**, 152–175.

Nicholson, P., French, R., McGhee-French, C., Hedman, M., Marouf, E., Colwell, J., Lonergan, K. & Sepersky, T. (2014b), 'Noncircular features in Saturn's rings II: The C ring', *Icarus* **241**, 373–396.

Rappaport, N., Longaretti, P., French, R., Marouf, E. & McGhee, C. (2009), 'A procedure to analyze nonlinear density waves in Saturn's rings using several occultation profiles', *Icarus* **199**.

Thomson, F., Marouf, E., Tyler, G., French, R. & Rappoport, N. (2007), 'Periodic microstructure in Saturn's rings A and B', *Geophysical Research Letters* **34**, L23203.